VIRAL DETERMINANTS OF H1N1 LAIV ATTENUATION IN HUMAN NASAL EPITHELIAL CELLS

by
Laura Canaday

A thesis submitted to Johns Hopkins University in conformity with the requirements for the degree of Master of Science

Baltimore, Maryland
April 2019

ABSTRACT

The influenza A virus H1N1 and H3N2 components of the live, attenuated influenza vaccine (LAIV) encodes HA and NA gene segments from circulating virus strains with the remaining gene segments derived from the cold-adapted master donor virus, A/Ann Arbor/6/1960 (H2N2). In addition to the temperature sensitivity mutations mapped to PB1, PB2, and NP, some studies demonstrate that the M segment can contribute to LAIV attenuation through an Ala to Ser mutation at M2 position 86 acquired during cold adaptation of A/Ann Arbor/6/1960; a mutation that is not found in any other influenza A virus strain. To test the hypothesis that the M2-S86A mutation contributes to LAIV attenuation, the M2-S86A mutation was introduced into LAIVs encoding H3N2 (A/Victoria/361/2011) or H1N1 (A/Michigan/45/2015) surface proteins and assessed the viruses' growth and replication characteristics. The results showed opposite effects, in which H3N2 LAIV replication increased, but H1N1 LAIV replication decreased. The overall replication of the H1N1 LAIV, regardless of insertion of the M2-S86A mutation, was significantly reduced compared to H3N2 LAIV. Because the failure of recent H1N1 LAIVs led to it being not recommended for use in the U.S. from fall 2016 - spring 2018, I also constructed a panel of H1N1 LAIVs encoding HAs of H1N1 vaccine strains from 2015-2018 and am assessing their ability to replicate in hNEC cultures and tolerate the M2 S86A mutations. These data indicate that the surface proteins may contribute to the attenuation of LAIV and therefore impact virus replication and vaccine efficacy.

Primary Advisor/Reader: Dr. Andrew Pekosz, PhD

Secondary Reader: Dr. Sabra Klein, PhD

ACKNOWLEDGEMENTS

I would first like to thank my thesis advisor, Dr. Andrew Pekosz, for the opportunity to work on a project that has reinforced my love of microbiology and reminded me why I am pursuing a career in science. His guidance and enthusiasm for virology and my project made working in the lab an absolute joy. I owe a huge thank you to Harrison Powell for taking the time to train me on everything I needed to know to be successful in the lab. His sage wisdom and begrudging friendship made working in the lab and navigating life in graduate school possible.

Thank you to all past and present members of the Pekosz laboratory, Emily (Thompson) Chavez, Allison Chen, David Jacobs, Kirsten Littlefield, Dr. Hsuan Liu, Dr. Alyssa McCoy, Dr. Farah El Najjar, Brendan Smith, Dr. Jason Westerbeck, and Siddhant Vyas, for your daily camaraderie, advice, and support. I would also like to thank Dr. Sabra Klein for her continued feedback and encouragement over the course of my projects. I need to thank the members of Dr. Klein's and Dr. Kim Davis's labs for their support and recommendations on my thesis work over the last 2 years.

A heartfelt thank you to my partner, Kevin McPartland, for being my biggest fan, my emotional rock, and my personal editor. Thank you for supporting my dreams and making long distance not as terribly awful as we thought it would be. Thank you to my parents, Clay and Lucy Canaday, for fostering my love of research, even though it meant moving farther away from home than before. Lastly, thank you to all the members of my ScM cohort, particularly Jordan Hoffman, Gaby Madrigal, Abeer Sayeed, and Kip Strother. Your friendships have made this entire experience better than I could have ever imagined.

CONTENTS

LIST OF TABLES AND FIGURES

TABLES……

FIGURES……..…….....

Chapter 1: INTRODUCTION

INFLUENZA

Influenza is a viral respiratory disease caused by influenza virus [1] . Influenza virus infects epithelial cells along the respiratory tract and has two main types of human concern, Type A (IAV) and Type B (IBV) [2]. Influenza virus is spread through inhalation by droplets made when someone coughs or sneezes or by fomites left on hard surfaces, ultimately ending up in the mouths or noses of nearby people [3]. IAV can be subtyped based on the surface proteins and categorized as either seasonal or pandemic.

PANDEMIC INFLUENZA

Pandemic influenza is caused by an IAV not previously seen in the human population [4]. The lack of preexisting immunity in the human population makes the magnitude of a pandemic much larger than that of seasonal influenza. Only four pandemics have been recorded over the last 100 years, occurring in 1918, 1957, 1968, and 2009. Due to the random nature of the emergence of pandemic influenza viruses, it is impossible to predict when the next pandemic will occur or how impactful it will be.

EPIDEMIOLOGY

The 1918 pandemic. Despite incredible advances made to understand the 1918 pandemic virus, the geographic and genomic origins of the virus remain unknown [5]. Analysis of RNA from preserved tissue samples of 1918 influenza cases showed some gene segments have a suspiciously high number of silent mutations from documented avian strains, while others remain deeply conserved. The contributing viruses had not circulated in humans or swine before the pandemic, making humans naïve to the entire

genome. In the United States, high influenza activity was first found in military camps in the spring of 1918, suspected to have been brought back from Europe after fighting in World War I [6]. In Europe, the early waves of disease were so mild, military officials did not take concern of it, not wanting to cause a panic. In the fall 1918, another wave of disease emerged out of an Army training camp outside of Boston and caused high fatality rates. Before the disease presented itself, soldiers were moved from Boston to Philadelphia and then to other bases all across the United States, spreading the deadly virus with them.

The 2009 pandemic. The first two cases of the 2009 H1N1 pandemic virus were recorded in Southern California in April 2009 [7]. Within one week, 10 other cases had been confirmed, and by June 2009, laboratory-confirmed cases were documented in over 70 countries [7]. The specific gene segments from this virus had never been previously reported in humans or animals, but the hemagglutinin (HA) surface protein gene was closely related to the HA from the 1918 H1N1 virus [8]. Upon serological analysis, data suggested this similarity provided older adults some cross-reactive protection against the virus, explaining the surprisingly low infection and death rates in the 65 and up population. Conversely, this left everyone under 65-years old immunologically naïve and highly susceptible to contracting the disease. The virus's genome was related to North American and Eurasian swine H1N1 viruses, with strong evidence suggesting the virus mutated in Central Mexico [9]. Further analysis showed that this virus was not circulating in the U.S. swine population, nor did the initial cases have exposure to pigs or each other [10]. Unlike the 1918 pandemic, surveillance systems were in place across the United

States to track how the virus was spreading, how it was affecting public health efforts, and to quickly characterize the new virus.

PUBLIC HEALTH CONCERNS AND IMPACTS

The 1918 Influenza pandemic was determined to be caused by an H1N1 IAV that came from avian origins [11]. Estimates predict that over one-third of the world's population was infected with the virus, killing 50 million people worldwide [11]. This pandemic saw a high rate of infection and death in the 20-40 year old age category, a population not typically affected by influenza with such severity.

After the 2009 H1N1 pandemic, the Centers for Disease Control and Prevention (CDC) reported that 60.8 million cases, 274,304 hospitalizations, and 12,469 deaths occurred in the United States solely from this novel H1N1 virus [11]. Working adults were found to have a risk of death 8-12 times greater than a typical influenza season, a trend also seen in the 1918 epidemic [12]. The 2009 season started earlier than normal, with cases of the new virus being reported in April, when typically, the season starts around October. The peak of hospitalizations also occurred earlier than normal in October into November, as opposed to January into February.

SEASONAL INFLUENZA

Seasonal influenza is caused by both IAV and IBV, and it typically circulates during the local winter months [4]. IAV viruses are subtyped based on their HA and NA proteins, and the current strains found in the human population are H1N1 and H3N2 viruses [13]. IBV viruses are not subtyped like H1N1 viruses but can be broken down based on lineages. Circulating human IBV are from the Yamagata and Victoria lineages. The structures and functions of IAV and IBV are extremely similar [14]. However, IAV

has a wide range of hosts, allowing for more reassortment events with novel proteins. This gives IAV a pandemic potential. Meanwhile, IBV's only known hosts are humans and seals, greatly limiting the pandemic potential.

EPIDEMIOLOGY

Unlike pandemic influenza virus, seasonal influenza virus cannot be traced back to a location or reservoir of origin. However, due to national surveillance infrastructure, the CDC is able to track "when and where influenza activity is occurring, influenza-related illness, determine what influenza viruses are circulating, detect changes in influenza viruses, and measure the impact influenza is having on hospitalizations and deaths" [15]. This data is recorded by location and age. A subset of viruses is tested further to characterize that season's circulating viruses, elucidate how it changed from the previous season, and determine how effective the approved vaccines are against it. Information is updated weekly to provide a working analysis of the viruses as the season progresses.

Additionally, influenza-associated deaths in children under 18 years old became a nationally notifiable condition in 2004 [15]. A pediatric death is defined as "a death resulting from a clinically compatible illness that was confirmed to be influenza by an appropriate laboratory diagnostic test" with "no period of complete recovery between the illness and death" [15]. Information about demographic, underlying conditions, co-infections, and location are also collected.

PUBLIC HEALTH CONCERNS AND IMPACTS

Due to the complexity of influenza surveillance, the CDC is only able to estimate how many cases and deaths influenza causes each season. They state the reason for

estimating is “to inform policy and communications related to influenza” [16]. Because influenza is not a nationally notifiable disease for adults, up to 50% of the population does not seek medical care for influenza-like symptoms, and not all influenza-driven deaths indicate influenza as the cause of death on death certificates [16]. These factors lead to underestimates of burden, therefore the CDC has developed models to estimate the national burden each season [17].

Aside from mortality, public health officials are interested in the burden of influenza because the illness can impact school and work attendance, daily productivity, and military capacity. Since 2010, the CDC estimates that influenza causes between 9.3 million and 49 million illnesses, 140,000 – 960,000 hospitalizations, and 12,000 – 79,000 deaths each year in the United States [18]. Current estimates, which are still being finalized, state that 49 million people presented symptomatic illness, 960,000 people were hospitalized, and 79,000 people died from influenza during the 2017-2018 season [18]. A study using 2003 hospitalization and death data estimate that “days of productivity lost due to illness” was 44 million days in 2003 [19]. Economically, the total economic burden of the influenza season in 2003 was $87.1 billion [19]. Of that, $16.3 billion was attributed to lost earnings due to lost productivity from illness and loss of life.

INFLUENZA VIRUS GENOME, DIVERSITY, AND REPLICATION

VIRION STRUCTURE

Influenza viruses belong to the *Orthomyxoviridae* family and utilize an 8-segment, single-stranded, negative sense RNA genome [14]. Specifically for IAV, the HA and neuraminidase (NA) surface glycoproteins and portions of the matrix (M) M2

ion channel are seen on the outside of the viral envelope. Moving inwards, M1 surrounds the virion core. NS2 and the ribonucleoprotein complex is composed of RNA segments coated by NP and the PB1, PB2, and PA proteins, forming the heterotrimeric RNA-dependent RNA polymerase are found internal to M1 [14].

ANTIGENIC DRIFT

Antigenic drift is change in the virus seen due to small changes over time as the virus replicates [20]. Typically, changes this small result in viruses that are closely related to each other and usually share antigenic properties. Over time, as the viruses continue to replicate, enough small changes can result in a virus a larger distance away from its predecessor. Due to the small changes, antigenic drift happens frequently. Antigenic drift is most relevant to the influenza HA and NA proteins, as antibodies to those proteins are associated with protection from disease.

ANTIGENIC SHIFT

Antigenic shift is a major change in the genome that results in HA or NA proteins that have not been seen in the human population becoming dominant in human influenza viruses [20]. These new surface proteins typically mean that there is little to no preexisting antibody immunity in the human population against them, allowing the virus to replicate with little immunological interference and being able to spread more freely than its predecessor virus. This is what generates pandemic influenza viruses. Because of the major change necessary, antigenic shifts only happen occasionally.

REPLICATION CAPACITY

Like any virus, influenza virus goes through the basic sequence of the viral replication cycle [14]. Viral attachment is facilitated by influenza virus HA recognizing sialic acid on the host cell surface. In humans, this is predominantly α-2,6 sialic acid. After attachment, the virus is endocytosed and uncoated. After being uncoated, ribonucleoproteins are moved to the host cell nucleus. In the nucleus, the viral negative sense RNA is used as a template to synthesize one positive-sense mRNA strand as a template for viral protein synthesis and one positive-sense cRNA strand to be used to generate more copies of negative-sense vRNA. The mRNA generates its own poly-A tail from a stretch of uracil residues on the vRNA and "cap snatches" from host pre-mRNA. The mRNA is ready to be exported and translated further. All 8 segments must be present in a new virion for the new virus to be infectious. Virus budding occurs at the cell membrane and is facilitated by the sialidase activity of NA, which prevents virus particles from clumping together or reattaching to the cell the particles budded from by removing sialic receptors from those cells and viruses.

To this end, in order for a virus particle to be infectious, it must contain all 8 genome segments. After a single round of replication across an array of IAV strains, of cells infected with a single virion of IAV, up to 90% released noninfectious particles [21]. In addition to the replication process necessary to generate infectious particles, defective interfering (DI) particles, noninfectious particles that carry an incomplete genome, have been found to inhibit infectious virus replication [22].

MATRIX PROTEIN

As previously stated, the M genome segment encodes 2 proteins, M1 and M2[14]. Despite being from the same genome segment, M1 and M2 have very different roles, which differ between IAV and IBV.

M1

The M1 protein is a 252 amino acid matrix protein that surrounds the inner surface of the virion membrane. It has lipid binding components and interacts with the cytoplasmic tails of the viral membrane proteins M2, HA and NA. M1 is the primary coordinator of viral budding [23]. HA has been shown to stimulate M1 binding to the virion membrane. M1 is able to regulate viral budding in the absence of M2 [24]. M1 can be associated with viral budding, regardless of whether a genome has been packaged.

M2

M2 proteins are 97 amino acid ion channel membrane proteins. It has been found that for every one M2 protein, there are anywhere from 10-100 HA proteins packaged into virions [14]. M2 has noted roles in viral entry, membrane scission, and infectious virus particle production [25]. M2 allows for the translocation of hydrogen ions into the virion interior and allows the vRNP dissociated from the viral membrane, facilitating transport to the host cell nucleus for replication [26]. Mutations in the M2 cytoplasmic tail, particularly changing the tyrosine at position 76, have shown decreases in virion infectivity, producing particles with reduced amounts of viral nucleoprotein and genomic RNA, and changes in virion morphology [24],[26]. When the distal tail of M2 is truncated, the number of infectious viral particles decreases significantly. During the cold adaptation process for LAIV generation, M2 mutated from an alanine to a serine at the

86th amino acid of master donor H2N2 strain. This mutation has been shown to contribute to the attenuation phenotype of LAIV on an H3N2 backbone and replicate lower on human nasal epithelial cells (hNECs) at 37°C [25].

HA

Hemagglutinin (HA) is a glycoprotein on the influenza virus surface that is responsible for receptor binding and membrane fusion [27]. Conserved residues in the head of the HA protein bind to sialic acids on host cells surfaces [27]. After the virus is bound to the receptor and the pH is lowered, HA mediates fusion of the virus membrane to the cell's endosomal membranes [28]. During this activation, HA undergoes a dramatic structural change, and where these changes occur characterize HAs into two groups [28]. As previously mentioned, human influenza viruses bind to α2,6-linked sialic acids, found predominantly in the human upper respiratory tract, while avian viruses preferentially bind to α2,3-linked sialic acid [28]. Swine, however, bind both kinds of sialic acid. Due to this, several pandemics, including the 2009 H1N1 pandemic, can be traced back to swine internal influenza proteins gaining human surface proteins and circulating in the naïve human population [29]. Mutations on HA can influence binding affinity and specificity by changing the sequence around the receptor-binding site, affecting the virus's ability to bind. Notably, a Q223R mutation on HA has shown increased replication in embryonated eggs by changing the binding preference from α2,6-linked sialic acids to α2,3-linked sialic acids [30]. An E47K mutation on the HA2 subunit on the stalk of HA, found in H1N1 viruses after 2009, has been found to stabilize HA, lower the required pH for fusion, and raise the acidic stability [31]. This resulted in higher thermal stability after high temperature treatment and increased infectivity in ferrets. In addition

to these kinds of mutations, generic antigenic drift mutations occur in HA and make annually updating the surface proteins of the vaccine viruses necessary.

INFLUENZA VACCINE

A vaccine against influenza virus has been available since 1933, but that first vaccine only contained one strain of IAV [32]. Current vaccines contain 4 different viruses, an IAV H1N1, IAV H3N2, IBV from the Yamagata lineage, and an IBV from the Victoria lineage [33]. The most common way influenza vaccines are manufactured is using an egg-based process regulated by the Food and Drug Administration [34]. CDC or a WHO Global Influenza Surveillance and Response System laboratories provide private manufacturers with the vaccine viruses that have been grown in eggs. The viruses are injected into embryonated hen's eggs, where they replicate. This process requires millions of eggs and a long time to generate the amount of virus necessary. Due to this lengthy process, the viruses to be used in the upcoming winter are selected in February, which limits the amount of research and surveillance CDC can conduct on circulating strains and may prevent the best virus from being selected.

There are 2 main compositions of influenza vaccines, which are based on how the viruses in the vaccine are generated- inactivated influenza vaccine (IIV) and live attenuated influenza vaccine (LAIV) [33].

INACTIVATED INFLUENZA VACCINE

As the name indicates, the IIV contains inactivated virus. The first inactivated vaccine was generated in the late 1930s, with widespread generation and use for the public starting in 1945 [32]. The vaccine was a military project for the U.S. to try and

protect troops going to Europe to fight in World War II. With that, the head of the U.S. Army Commission, Thomas Francis, decided to try vaccines generated from virus grown in hen's egg allantoic fluid, following Burnet's methods, purified, and formalin inactivated [32]. Using both an IAV and IBV, that vaccine displayed up to 69% efficacy. Since then, the bivalent vaccine has been developed into a quadrivalent vaccine and 10,000 doses to over 100 million doses [33].

The vaccine contains primarily HA and NA proteins, which elicit local and systemic immune responses with the antibody response peaking two weeks after vaccination and dominated by IgG [35]. Most IIVs are unadjuvanted and are administered via intramuscular injection [33]. In the United States, IIVs are recommended annually for anyone over 6 months old [33]. IIVs display anywhere from 10% to 60% efficacy, averaging around 41% over the last 14 years across all age ranges [36]. In the 2017-2018 season, adults were found to have a vaccine coverage of 37.1%, the lowest coverage in seven seasons [37]. The rate of vaccination increased with age, as 26.9% of 18-49 year olds were immunized while 59.6% of adults over 65 years old were covered [37]. As for children, ages 6 months through 17 years old, coverage during the 2017-2018 season was 57.9%, 1.1% lower than the previous season [38]. Unlike adults, vaccination coverage decreased as age increased [38]. From September 2017 through February 2018, approximately 155.3 million doses of vaccine were distributed in the United States [33].

LIVE ATTENUATED INFLUENZA VACCINE

Similarly, as the name indicates, the live attenuated influenza vaccine (LAIV) contains live, replicating influenza viruses that have been weakened, or attenuated, to

prevent illness. The live viruses in the vaccine allow for replication after immunization, to elicit a longer, more robust immune response [39]. Influenza virus was first cold adapted to grow at 25°C during the 1960s [40]. The IAV strain used, A/Ann Arbor/6/60, is an H2N2 virus that grows at the suboptimal temperature of 25°C, is unable to replicate above 39°C, sheds infectious virus at low levels in human pharyngeal secretions, but does not transmit between humans [40]. It is worth noting, that the upper portion of the human respiratory tract, including the nasal passageways, is at a temperature of 32°C, while the core body temperature, including the lower portion of the respiratory tract, is 37°C. Mutations in the gene segments from the cold adaption process account for the genetic stability of the virus and helped designate it as the "master donor virus" (MDV) for all human LAIVs. However, cold adapting each season's circulating virus would not be efficient, so the internal gene segments of A/Ann Arbor/6/60, which contain the genetic determinants controlling temperature sensitivity and attenuation, are reassorted with the HA and NA segments of the circulating strain to generate a 6:2 reassortant virus [40]. This allows for the relevant surface proteins to elicit an immune response to protect against the currently circulating strains, while the cold-adapted internal genes provide consistent machinery for replication in the nasal passageway. Around the same time, another H2N2 MDV was being developed in Russia, A/Leningrad/134/57 [41]. An LAIV prophylaxis against influenza has been used in Russia since 1987. Additionally, however, A/Leningrad has been under study as a potential H5N1 and H7N9 pandemic LAIVs [41].

The LAIV used in the U.S. is manufactured by MedImmune and marketed as "FluMist® Quadrivalent" [42]. The trivalent form of FluMist was first approved for use by the FDA in June 2003 [43]. In both adults and children, prior to 2009, the LAIV

showed less confirmed cases of influenza and more antibody cross reactivity [44],[45]. The vaccine itself is administered intranasally by a prefilled, single-use sprayer [42]. This intranasal vaccination generates an immune response that more closely resembles a natural immune response when compared to an intramuscular injection [39]. The lack of injection is very appealing for children, however, the LAIV is only licensed for persons older than 2 years ~~old~~. The number of children able to receive the LAIV is also limited by a list of contraindications, including children and adolescents receiving an aspirin- or salicylate-containing therapy, children between 2-4 diagnosed with asthma, any child who is immunocompromised, and those with a history of Guillain-Barré syndrome [42]. Before 2009, FluMist had superior efficacy in children, aged 6 -71 months, when compared to that same season's IIV [46],[43]. FluMist and the IIV demonstrated statistically significant and comparable protection against medically attended influenza during the seasons starting in 2010, 2011, and 2012 [43]. An analysis of children presenting to outpatient settings with influenza like illness during the 2015-2016 influenza season showed that 10% of the total children enrolled in the study received the LAIV, while 31% received the IIV, and 59% were unvaccinated [47].

However, FluMist was pulled from the US market before the 2016 influenza season due to poor to nonexistent effectiveness starting in the 2013 season, which studies later revealed was due to a faulty H1N1 component, an HN1pdm09-like virus [48]. That season, the IIV displayed 60%-74% protection against an A/H1N1pdm09 virus, while FluMist only showed 13-17% effectiveness [43]. The surface proteins of the H1N1 component were changed so dramatically after the 2009 pandemic, that subsequent vaccine H1N1 viruses did not match the circulating virus, rendering a useless vaccine

virus [46]. Despite a faulty H1N1 component, the H3N2 and IBV components showed similar effectiveness against those strains as the IIV [46]. A similar trend was seen during the 2015-2016 season as well, causing the Advisory Committee on Immunization Practices (ACIP) to remove FluMist from U.S. markets before the 2016 season [43]. It is worth noting, that during this time, consistent effectiveness was seen for the LAIV outside the U.S. [43]. Luckily, a non-significant decrease was seen in the number of children vaccinated the two seasons that FluMist was off the market, when compared to children vaccine by both IIV and FluMist the seasons before 2013 [38].

However, after changing the H1N1 component and adding additional efficacy tests, the ACIP approved the LAIV to return to the US markets for the 2018-2019 season [48]. The new A/Slovenia H1N1strain has displayed increased replication in nasal epithelial cultures and better capability to go through multiple rounds of replication, unlike the A/Bolivia predecessor [43].

THESIS OBJECTIVES

In this thesis, I have studied the role of three aspects of LAIV that are rarely considered during the generation of seasonal LAIV. First, is the contribution of a mutation at position 86 of the M2 protein to the ability of LAIVs encoding either H3N2 or H1N1 surface proteins to replicate in a temperature dependent manner. The attenuation of LAIV is hypothesized to be mediated by its internal gene segments, which are conserved irrespective of the surface proteins on that virus. Second, the effect of specific surface proteins on the replication of LAIV, which is often overlooked as it is assumed that any HA or NA can mediate effective LAIV replication and does not contribute to virus attenuation. Finally, the use of human nasal epithelial cells (hNECs) as a surrogate system to study LAIV replication in order to test LAIV replication in an environment that most resembles the human upper respiratory tract. My research has shown important, previously overlooked contributions of all three to LAIV replication and attenuation.

Chapter 2: CHARACTERIZATION OF M2 MUTATED VIRUSES

BACKGROUND

M2 in an integral membrane protein required for virus entry, membrane scission, and infectious virus particle production [25]. M2 forms disulfide-linked homo-tetramers with pH-gated, proton-selective ion channel activity critical for virus uncoating [25]. Studies show that when the M2 cytoplasmic tail is truncated by 16 amino acids, infectious virus particle production is decreased, but when only the last 8 amino acids are truncated, infectious virus particle production is not changed [49]. Similarly, when the last 8 amino acids (M2 82-89) were mutated to alanine residues, infectious particle production was unchanged. However, M2-83 and M2-86 were unaltered due to having alanine residues before the mutations. A86 is highly conserved across human influenza viruses, except for 2009 pandemic H1N1 viruses, where it is a Valine, and LAIV viruses, which contain a Serine [25]. This chapter focuses on experiments to determine how mutating the 86th amino acid from the LAIV WT *Ser* to the pre-cold adaptation *Ala* affects H1N1 LAIV virus replication as compared to H3N2 LAIV.

MATERIALS AND METHODS

PLASMIDS

The internal plasmid of pHH21 M LAIV encodes the entire influenza H2N2 A/Ann Arbor/6/60 M segment under control of the human RNA polymerase I promotor and murine RNA polymerase I terminator [50]. Mutations were introduced to the plasmid using the QuikChange Lightning site-directed mutagenesis (Agilent, Santa Clara, CA) protocol. The sequences of the forward and reverse mutagenesis primers used to introduce the S86A mutation are in Table 1 (M2_S86A_1 and M2_S86A_2).

Using Dpn1 enzyme for digestion, the parental DNA was removed from the PCR product, and the product was transformed into competent bacterial (DH5α) cells. DNA from multiple bacterial clones was extracted using QIAprep Spin Miniprep Kit (Qiagen). Using an LAIV M segment-specific primer, H2N2 LAIV Mseq 660F (Table 1), the DNA was sequenced for the appropriate mutations.

CELL LINES

Madin Darby canine kidney (MDCK) and human embryonic kidney 293T (293T) cells were cultured in Dulbecco's Modified Eagle Medium (DMEM, Sigma-Aldrich) with 10% fetal bovine serum (FBS, Gibco Life Technologies), 100U penicillin/mL with 100μg streptomycin/mL (Quality Biological), and 2mM L-Glutamine (Gibco Life Technologies) at 37°C with air supplemented with 5% CO_2.

Human nasal epithelial cell (hNEC) cultures were isolated from non-diseased tissue after endoscopic sinus surgery for non-infection related conditions [25]. The cells were collected from 4 female patients. The cells were differentiated at an air-liquid

interface (ALI) in 24-well Falcon filter inserts (0.4-μM pore; 0.33cm^2; Becton Dickinson) before infection, using ALI medium as basolateral medium.

REVERSE GENETICS

Recombinant viruses were rescued using a 12 plasmid reverse genetics system [50]. All eight segments of the target virus are required, in addition to helper plasmids encoding viral replication machinery. 293T cells were infected with 0.5μg of pHH21 plasmids encoding A/Ann Arbor/6/60 LAIV internal genes PB2, PB1, PA, NP, NS, and the WT and M2-S86A mutant M. 0.5μg of A/Michigan/45/2015 HA and NA in the pHH21 plasmid were added to supply the surface proteins. Additionally, 1μg of protein expression plasmids for A/Udorn/72 PB2, PB1, and NP plus 0.2μg PA were added as plasmids that would reconstitute the influenza polymerase activity. When the 8 target virus plasmids infect the 293T cells, their corresponding vRNA is produced but unable to be replicated. The polymerase-containing replication machinery in the helper plasmids allow the vRNA to be replicated to produce more infectious virus particles.

TransIT-LT-1 (LT1) (Mirus, Madison, WI), a transfection reagent, was mixed with OptiMEM medium (Gibco, Carlsbad, CA) and incubated at room temperature for 15 minutes at a ratio of 2uL LT1 to 1ug plasmid DNA. The 12 plasmids were added to the solution and incubated at room temperature for 15 minutes. Complete medium was removed from 293T cells in 6-well plates and replaced with 2mL OptiMEM. The LT1-OptiMEM-plasmid solutions were then added to each well. The plates were incubated at 32°C with 5% CO_2 for 24 hours. N-acetyl trypsin (NAT) (Sigma, St. Louis, MO) was added to a final concentration of 10ug/ml to each well, and the plates were incubated for another 4 hours at 32°C with 5% CO_2. $5x10^5$ MDCK cells in 100uL infection medium

were added to each well, and the plate was incubated at 32°C with 5% CO_2. 1mL of transfected cell supernatant was collected and replaced with 1mL DMEM with 4ug/ml NAT, 100u/ml penicillin 100ug/ml streptomycin, 2mM L-Glutamine and 0.5% bovine serum albumin (BSA) (Sigma) (infectious medium with NAT, IM+NAT) daily until obvious signs of cytopathic effect were visible.

SEQUENCING

After plasmid, seed stock, and working stock generation, Sanger sequencing was utilized to confirm the appropriate M2-86 amino acid was in each virus. The sequencing was done at the Synthesis & Sequencing Facility of the Johns Hopkins University (Baltimore, MD) using Applied Biosystems 3730xl DNA Analyzer and dye terminator sequencing technology. DNA plasmid concentration was found using the NanoDrop spectrophotometer ND-1000 (Thermo Fisher Scientific). The primer H2N2 LAIV Mseq 660F (Table 1) was used.

SEED STOCKS AND WORKING STOCKS

To generate seed stocks, fully confluent 6-well plates of MDCK cells were washed 2 times with PBS+ and then infected with 250µL of the plaque pick solution for 1 hour, with redistribution every 15 minutes, at 32°C with 5% CO_2. After 1 hour, the infection media was removed and 2mL of IM+NAT (1:1000) was added. Virus supernatant was collected with 75% of the cells showed cytopathic effect, typically 5 days post-infection. The seed stocks were titrated via $TCID_{50}$ assay. Working stocks were generated from seed stocks, in a similar fashion, except on fully confluent MDCK cells in 75cm^2 flasks, and the seed stock inoculum was diluted to an MOI of 0.001 in IM.

PLAQUE ASSAY

Plaque assays were performed in 90-100% confluent 6-well plates of MDCK cells. 250μL of serial 10-fold dilutions of transfection supernatant in IM+NAT (1:1000) were added to each well, and incubated at 32°C, for plaque picking or plaque morphology studies, or 37°C, for plaque morphology only, with 5% CO_2 for one hour, with gentle distribution of the solution every 15 minutes. Wells were then covered with 2% agarose combined with 2X MEM plus 1:1000 NAT. Once the agarose solidified, plates were incubated at 32°C, for plaque picking or plaque morphology studies, or 37°C, for plaque morphology only, with 5% CO_2 for 5 days. After 5 days, one of two protocols was followed. Plaques could be picked using a 1mL blunt pipette tip, added to tubes containing IM, and stored at -80°C to be used to establish seed stocks of the virus colony. Alternatively, plates could be fixed with 4% formaldehyde in PBS overnight and stained with Napthol Blue Black overnight to be used to quantify plaque size and morphology.

To quantify plaque area, images of the wells were captured using a dissecting microscope with an Olympus DP-70 color camera. A standard ruler image was also taken to set a reference. Photos were opened in ImageJ (NIH), a reference length of 1cm was measured via the ruler image, and borders were drawn around individual plaques using the Freehand selector. Measurements of the area of the plaque were calculated in ImageJ, and data was graphed and analyzed in GraphPad Prism 8 (GraphPad Software, San Diego, CA).

$TCID_{50}$ ASSAY

Fifty percent tissue culture dose ($TCID_{50}$) was determined in 96-well plates of 90-100% confluent MDCK cells. After being washed twice with PBS+, ten-fold serial

dilutions of the viruses in IM+NAT (1:1000) were made, and 20µL of each dilution was added to 6 wells. The plates were incubated at 32°C with 5% CO_2 for 7 days. The cells were fixed with 4% formaldehyde (Fisher Chemical) in PBS for at least 1 hour and then stained with Napthol Blue Black solution overnight. Endpoint values were calculated by the Reed-Muench method [51].

LOW MULTIPLICITY OF INFECTION (MOI) GROWTH CURVES (GC)

Low MOI GCs were used to determine viral growth kinetics. The low MOI promoted multiple rounds of virus replication, thereby optimizing the detection of replication differences between virus strains. An MOI of 0.01 was used in MDCK cells and 0.1 in hNECs. For MDCK cell infections, 100% confluent 24-well plates of MDCK cells were washed 3 times with PBS+. The virus inoculum was diluted in IM, 100µL was added to the cells, and allowed to incubate at 32°C or 37°C for 1 hour, with redistribution every 15 minutes. The inoculum was removed, the cells were washed 3 times with PBS+ and incubated with 500µL of IM+NAT (1:1500). At the indicated times, all media was collected and fresh IM+NAT was re-supplemented.

For hNEC cell infections, fully differentiated 24-well plates with a transwell membrane had their basolateral media replaced and were washed 3 times on the apical side with IM, with a 10 minute 32°C or 37°C with 5% CO_2 incubation between each wash. The virus inoculum was diluted in IM, 100 µL was added to the cells, and allowed to incubate at 32°C or 37°C for 2 hours. The inoculum was removed, the cells washed 3 times with PBS+ and incubated at 32°C or 37°C with 5% CO_2. At the indicated times, IM was added to the apical side, allowed to incubate at the corresponding temperature for 10 minutes, and then collected. Basolateral media was collected and replaced every 48

hours. Infectious virus particle production was quantified using a $TCID_{50}$ on MDCK cells.

RESULTS

Rescue of recombinant influenza viruses encoding M2-S86A mutations

The A/Ann Arbor/6/1960 (H2N2) LAIV M2 protein contains an Alanine to Serine mutation at position 86 of the M2 cytoplasmic tail, which was acquired during the cold adaptation process of the virus [52]. Recombinant A/Michigan/45/2015 H1N1 viruses expressing either LAIV M2-WT or LAIV M2-S86A were successfully generated. The entire coding region of the M segment of each virus was sequenced to confirm the expression of the desired mutation and to verify no other amino acid mutations were present.

Recombinant A/Victoria/361/201 H3N2 viruses expressing either LAIV M2-WT or LAIV M2-S86A were successfully generated previously in the lab [25]. Working stocks of these viruses were re-titered and had the entire coding region of the M segment re-sequenced to confirm the expression of the desired mutation and to verify no other mutations occurred during the freeze-thaw cycle since the viruses' last use.

Plaque assay of viruses containing WT and S86A M2

To determine how this mutation may affect virus replication at each temperature, plaque assays were performed to study plaque morphology and size on MDCK cells. Both H1N1 viruses were able to form plaques at both 32°C and 37°C **(**Fig. 1**,** Fig. 2**)**. The area of individual plaques for each virus at each temperature was calculated. At both temperatures, rMich-LAIV M2-WT had significantly smaller plaques than is rMich-LAIV M2-S86A counterpart. This result indicates that the serine mutation only seen in the LAIV strain of H1N1 negatively impacts plaque formation and viral replication.

Previous rVic-LAIV M2-WT and rVic-LAIV M2-S86A plaque assays did not inoculate the cells at the different temperatures. The method I used would show how well these viruses are able to infect the cells at the temperature they would ultimately be incubated at as well. Both viruses were able to form plaques at both 32°C and 37°C (Fig. 3, Fig. 4). The area of individual plaques for each virus at each temperature was calculated. At both temperatures, rVic-LAIV M2-WT had significantly larger plaques than its rMich-LAIV M2-S86A counterpart. This result indicates that the serine mutation only seen in the LAIV strain of H1N1 positively impacts plaque formation and cell-to-cell spread. This is the opposite phenotype of that seen in the H1N1 rMich viruses.

Replication of recombinant viruses at 32°C

To evaluate the viruses' growth kinetics and ability to survive multiple rounds of replication, multistep low MOI growth curves of both viruses were performed on MDCK cells and differentiated hNECs at 32°C to replicate the temperature of the upper portion of the human respiratory tract.

On MDCK cells, all 4 recombinant viruses reached a peak infectious virus titer at 48 hours post infection **(**Fig. 5**,** Fig. 6**)**. rMich-LAIV M2-WT reached and sustained its highest titer faster and longer than rMich-LAIV M2-S86A, while the differences between the viruses was slightly less than 10-fold, the differences were statistically significant. In contrast, there were no statistically significant differences between rVic-LAIV M2-WT and rVic-LAIV M2-S86A. When the H1N1 viruses are compared to the H3N2 viruses, the H3N2 viruses' peak viral titers were 1 to 1.5 logs higher than the M2-WT and M2-S86A H1N1 viruses, respectively (Fig. 10). These data suggest there is a slight effect of

M2-S86A on the replication of H1N1 LAIV but not on H3N2 LAIV at 32°C in MDCK cells.

In hNEC cultures, rMich-LAIV M2-WT reached its highest titer by 48 hours post infection, while rMich-LAIV M2-S86A peaked at 72 hours post infection (Fig. 7). The difference between the peak titers of the two viruses was 10-fold, with rMich-LAIV M2-WT having the higher titer. Over the course of the assay, rMich-LAIV M2-WT had over a 10-fold higher titer than rMich-LAIV M2-S86A. In contrast, both H3N2 viruses reached their peak viral titers at 72 hours post infection, with rVic-LAIV M2-S86A reaching an ultimately higher viral titer than its counterpart, but this difference was less than a 10-fold difference (Fig. 8). The kinetics of these viruses was similar, with rVic-LAIV M2-WT only reaching a higher titer at 72 hours post infection. Once again, the data show that M2-S86A has an effect in H1N1 LAIV but not in H3N2 LAIV, indicating the surface proteins can mediate a differential effect of the M2-S86A on LAIV replication.

The H3N2 viruses showed standard growth kinetics at 32°C on hNECs, with high amounts of infectious virus particle production between 12 and 72 hours post infection, while the H1N1 viruses reached significantly lower peak titers and never had a dramatic increase in infectious virus particle production in those first time points (Fig. 9). The difference in peak titers between the H3N2 viruses and the H1N1 viruses was over 1000-fold, despite having similar inoculation titers.

These data show that at 32°C, the mutation does not play a significant role on immortalized cells for either the H1N1 or H3N2 viruses. But in a human physiologically relevant model, this mutation might be to the fitness benefit of the H1N1 virus at 32°C,

while conferring not advantages for either H3N2 virus. This also started to elucidate a potential difference in the H1N1 viruses' abilities to replicate on our primary cell line.

Replication of recombinant viruses at 37°C

In addition to growth curves at 32°C, low MOI growth curves were performed on MDCK cells and in differentiated hNEC cultures at 37°C. The lower portion of the human respiratory tract and core human body temperature sits around 37°C, and growth curves at this temperature would elucidate any potential temperature sensitivity this mutation is responsible for.

On MDCK cells, both H1N1 viruses reached a peak viral titer at 48 hours post infection (Fig. 11). The two viruses replicated with similar kinetics and to similar titers over the course of the assay. The H3N2 viruses, however, reached their peak viral titer at 36 hours post infection (Fig. 12). While they both had similar titers leading up to their peak titer, rVic-LAIV M2_S86A sustained a significantly higher titer level from 36 hours post infection on over rVic-LAIV M2-WT. However, this difference was only about half a log. Even though the H1N1 viruses and H3N2 viruses reached their peak titers at different times, they all peaked around the similar titers, with the exception of rMich-LAIV M2-S86A, which was about 10-fold lower than either H3N2 virus (Fig. 16).

On hNEC cultures, rMich-LAIV M2-WT reached a peak viral titer at 36 hours post infection, but viral titer went below the limit of detection by 72 hours post infection. rMich-LAIV M2-S86A produced even less infectious virus and fell below the limit of detection by 24 hours post infection (Fig. 13). While the two viruses started at similar inoculums, their ability to replicate in hNEC cultures is drastically different. The H3N2 viruses, meanwhile, had very standard growth kinetics, with peak viral titer occurring for

both viruses at 72 hours post infection (Fig. 14). Unlike at 32°C, the difference between these peak titers was over 10-fold higher for rVic-LAIV M2-S86A and statistically significant. Throughout the most of the assay, rVic-LAIV M2-S86A had a 10-fold higher titer over rVic-LAIV M2-WT. This result is similar to what was previously published. Despite having similar inoculum titers, the H1N1 viruses are significantly worse at replicating on hNEC cultures at 37°C than when compared to the H3N2 viruses (Fig. 15). While the H1N1 viruses both fell below the limit of detection, the H3N2 viruses had not reached their peak titer yet. This was another indicator of these particular H1N1 surface proteins' lack of capability to replicate on a physiologically relevant human model. The data also indicate that the effect of the M2-S86A mutation can be very different depending on the HA and NA proteins encoded by the LAIV.

Replication of similar recombinant viruses at different temperatures

As for each virus compared to its temperature different assay, on MDCK cells, rMich-LAIV M2-WT reached higher titers at 32°C than 37°C, which is to be expected due to the temperature sensitive phenotype of the LAIV virus (Fig. 5, Fig. 11). Both assays reached a peak titer at 48 hours post-infection and had similar decreases in replication after that. The same trend was found in the rMich-LAIV M2-S86A viruses, with peak titer being reached at 48 hours post infection and close to a 10-fold decrease in titer for rMich-LAIV M2-S86A viruses grown at 37°C was observed (Fig. 5, Fig. 11). This ensures that our temperature sensitive phenotype was held within the recombinant viruses. Both H3N2 viruses reached their peak viral titers at different time points at the same temperature on MDCKs, 48 hours post infection at 32°C and 36 hours post infection at 37°C, the same trend of the viruses grown at 32°C reaching a higher peak

titer was seen (Fig. 6, Fig. 12). However, the difference in peak titer between the temperatures was less than a 10-fold difference for both viruses, suggesting that the surface proteins may be modulating the temperature dependent replication of LAIV. Both H3N2 M2-WT viruses reached a higher peak titer, about 10-fold higher, than its H1N1 M2-WT counterpart at the same temperature (Fig. 10, Fig. 16). The same trend is seen for the M2-S86A viruses, with H3N2 viruses grown at either temperature reaching a higher titer than its H1N1 counterpart at that same temperature (Fig. 5, Fig. 6, Fig. 11, Fig. 12).

On hNEC cultures, we see that both rMich-LAIV M2-WT and rMich-LAIV M2-S86A viruses replicate to significantly higher titers at 32°C than at 37°C (Fig. 7, Fig. 13). However, both viruses had very different growth kinetics at both temperatures. rMich-LAIV M2-WT peaked at different points during the assay between the temperatures and had over a 10-fold difference in peak titer. rMich-LAIV M2-S86A had over a 100-fold difference between peak titers, with the virus unable to replicate at 37°C. As for the H3N2 viruses, all the viruses reached their peak titers at the same time at both temperatures at 72 hours post infection. rVic-LAIV M2-WT grown at 37°C had over a 2.5-log decrease in peak titer compared to when it was grown at 32°C (Fig. 8, Fig. 14). rVic-LAIV M2-S86A had a 2-log difference between the viruses grown at 32°C and 37°C, with the viruses at 32°C reaching the higher titer. Similar to the H1N1 viruses, this keeps wells with the temperature sensitive phenotype seen in LAIV viruses. The peak titer for rVic-LAIV M2-WT at 32°C was over 1000-fold higher than the peak titer than rMich-LAIV M2-WT's peak titer, and the peak titer at 37°C was over 100-fold higher for the H3N2 M2-WT virus than the H1N1 M2-WT (Fig. 9, Fig. 15). The peak titers for the M2-S86A viruses were 4.5-logs different at 32°C, with the H3N2 virus generating more

infectious virus particle (Fig. 7, Fig. 8). At 37°C, the H3N2 M2-S86A virus replicated over 5-logs higher, but that is also due to the fact that the H1N1 M2-S86A virus did not replicate at all (Fig. 13, Fig. 14).

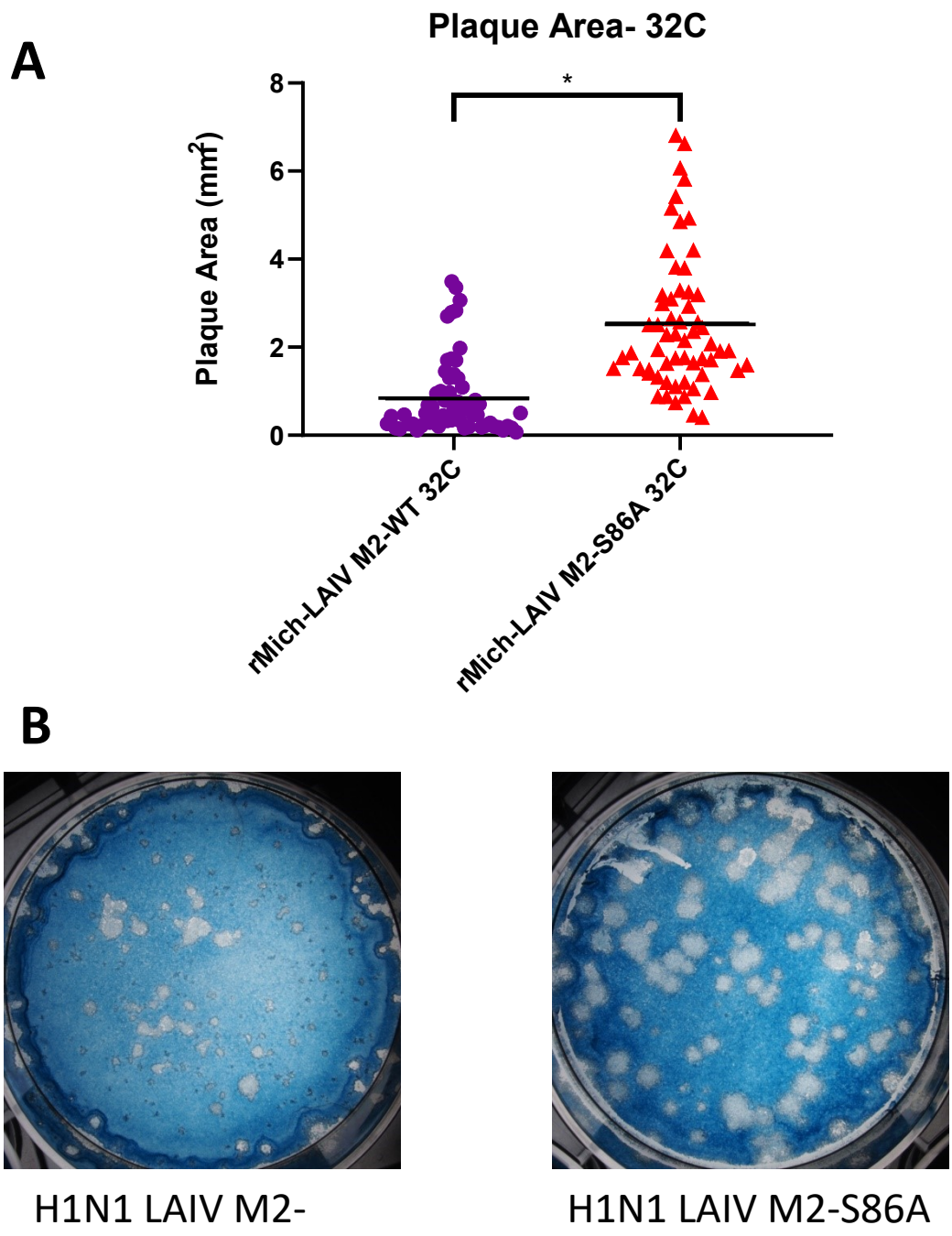

Fig. 1- Plaque Assay at 32°C. Plaque assays performed with indicated virus at 32°C. (A) Plaque area was calculated and individual plaque area and mean (crossbar) are shown. Significance determined with an unpaired t-test, *p<0.05. At least 60 plaques were quantified per virus. (B) Plaque morphology of recombinant influenza A viruses encoding mutations at M2 position 86.

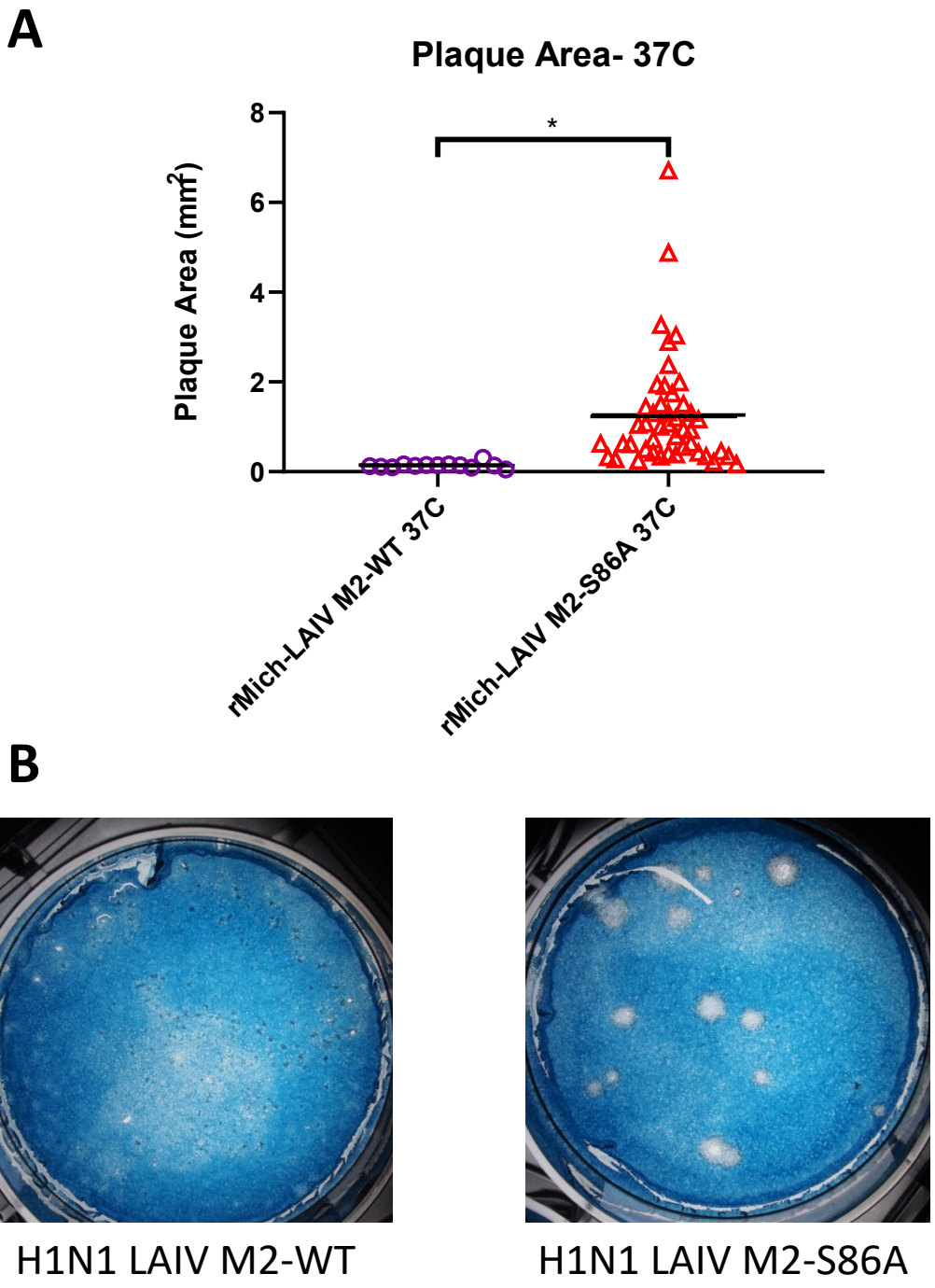

Fig. 2- Plaque Assay at 37°C. Plaque assays performed with indicated virus at 37°C. (A) Plaque area was calculated and individual plaque area and mean (crossbar) are shown. Significance determined with an unpaired t-test, *$p<0.05$. At least 60 plaques were quantified per virus. (B) Plaque morphology of recombinant influenza A viruses encoding mutations at M2 position 86.

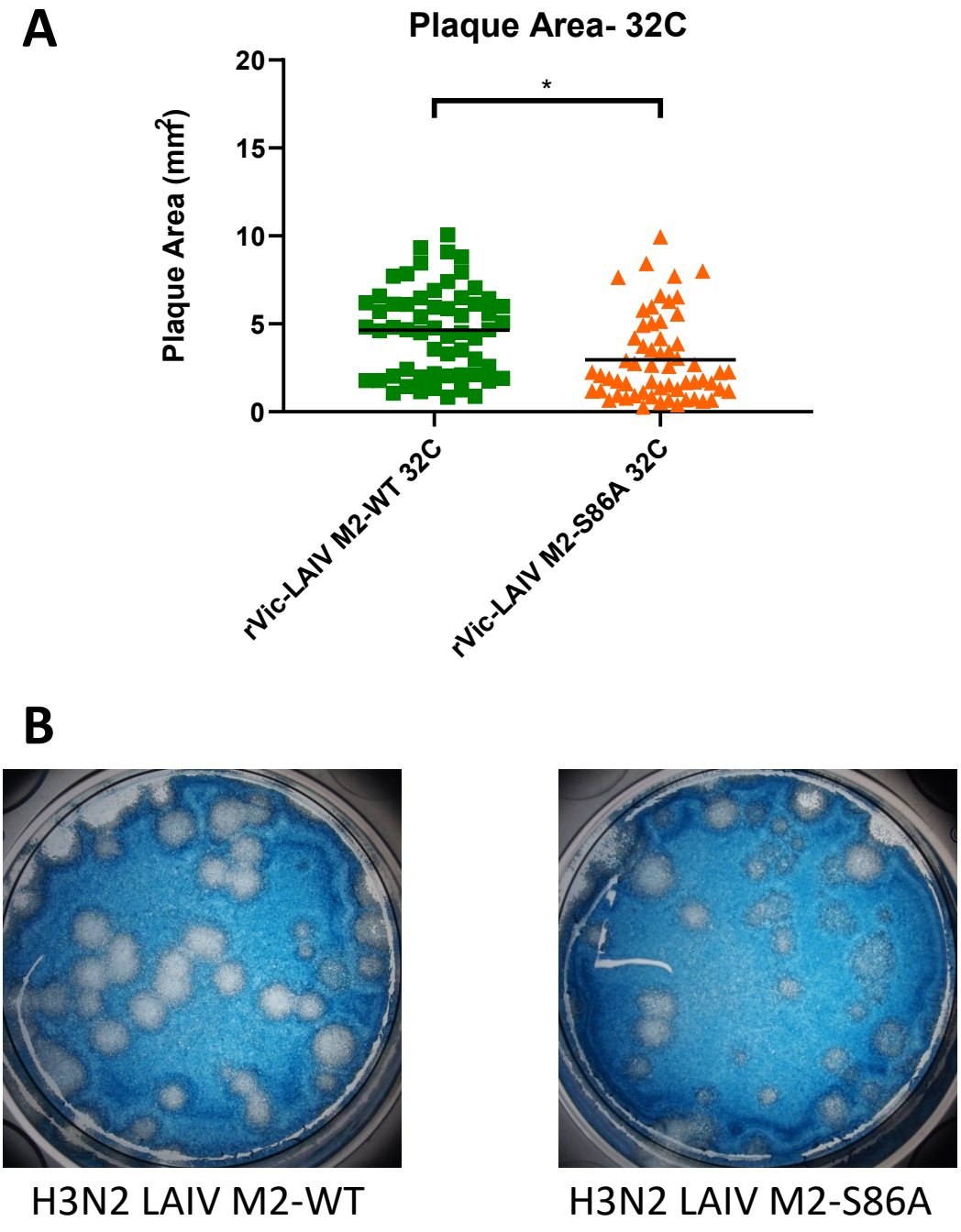

Fig. 3- Plaque Assay at 32°C. Plaque assays performed with indicated virus at 37°C. (A) Plaque area was calculated and individual plaque area and mean (crossbar) are shown. Significance determined with an unpaired t-test, *p<0.05. At least 60 plaques were quantified per virus. (B) Plaque morphology of recombinant influenza A viruses encoding mutations at M2 position 86.

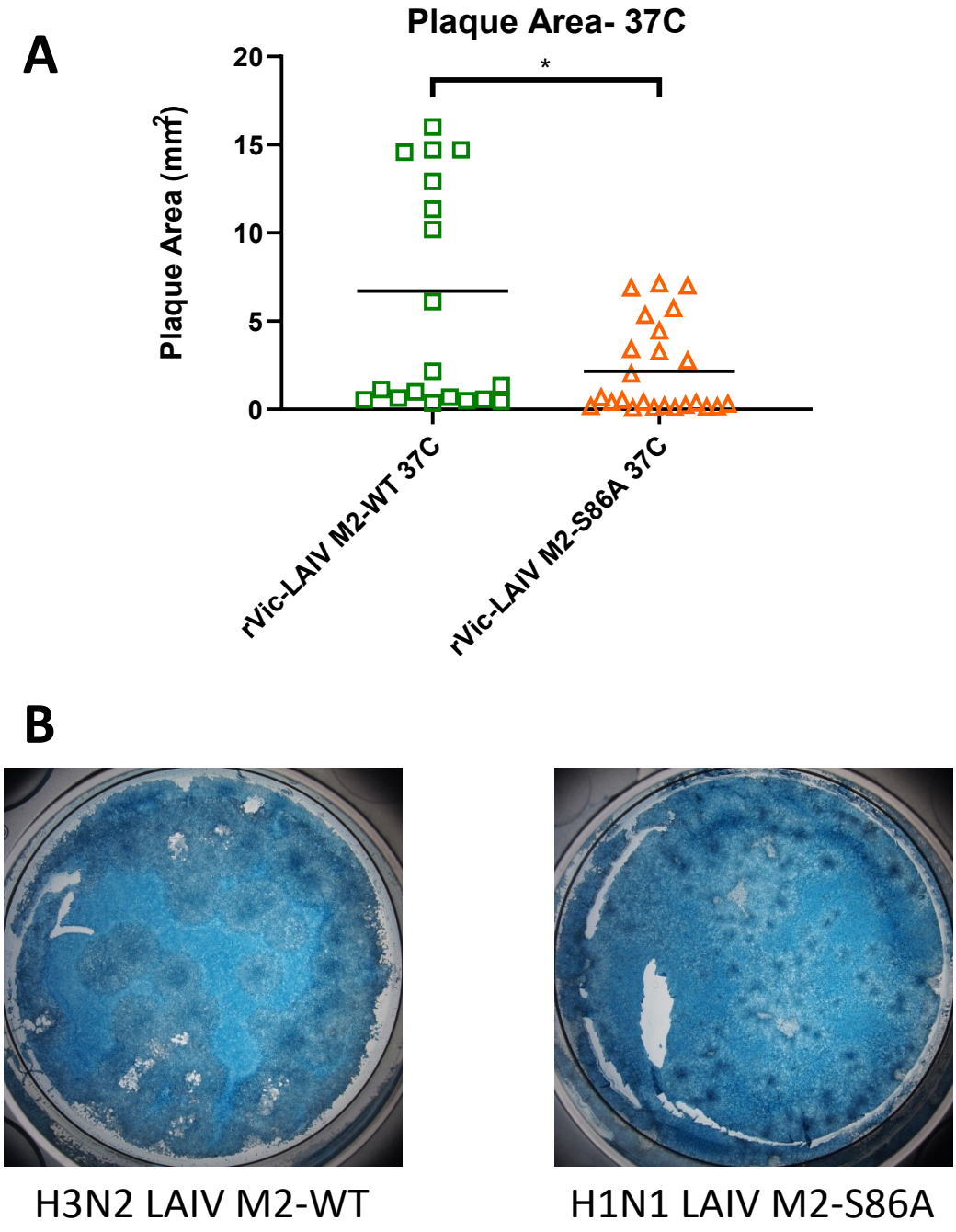

Fig. 4- Plaque Assay at 37°C. Plaque assays performed with indicated virus at 37°C. (A) Plaque area was calculated and individual plaque area and mean (crossbar) are shown. Significance determined with an unpaired t-test, *$p<0.05$. At least 60 plaques were quantified per virus. (B) Plaque morphology of recombinant influenza A viruses encoding mutations at M2 position 86.

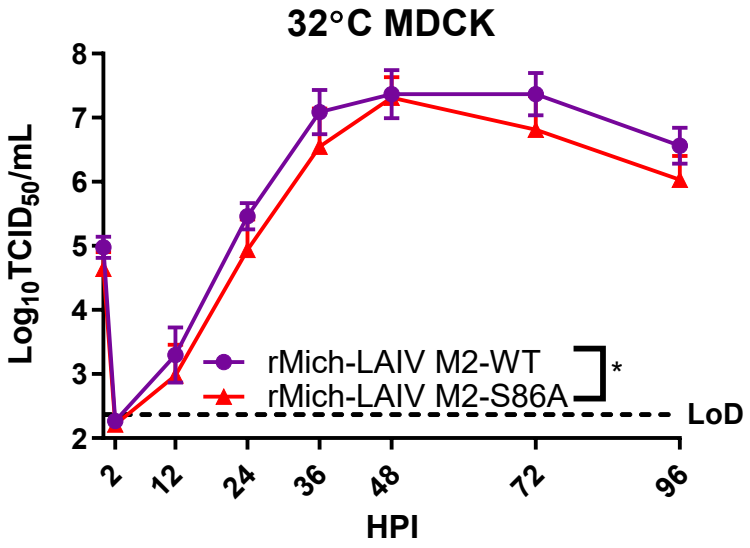

Fig. 5- 32°C H1N1 MDCK GC. A multi-step growth curve was performed on MDCK cells with the indicated H1N1 recombinant viruses at 32°C with an MOI 0.01. Statistical significance was measured with a two-way ANOVA followed by Bonferroni post-test. Results are from 3 independent experiments, each with 4 technical replicates. *p<0.05.

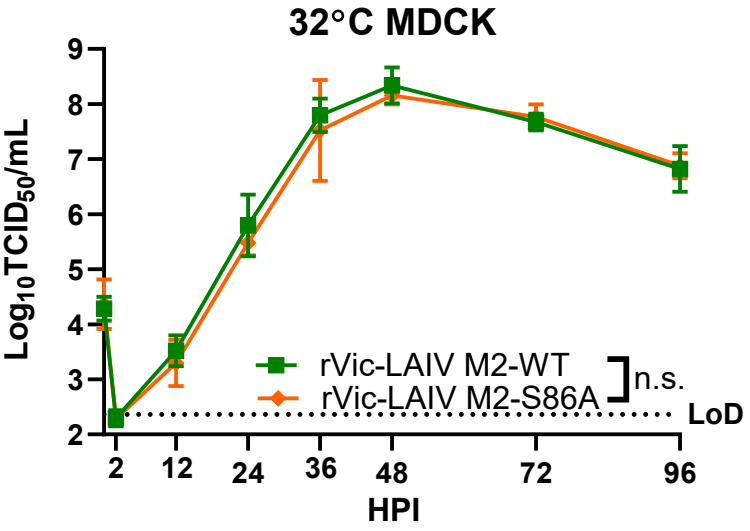

Fig. 6-32°C H3N2 MDCK GC. A multi-step growth curve was performed on MDCK cells with the indicated H3N2 recombinant viruses at 32°C with an MOI 0.01. Statistical significance was measured with a two-way ANOVA followed by Bonferroni post-test. Results are from 3 independent experiments, each with 4 technical replicates. *p<0.05.

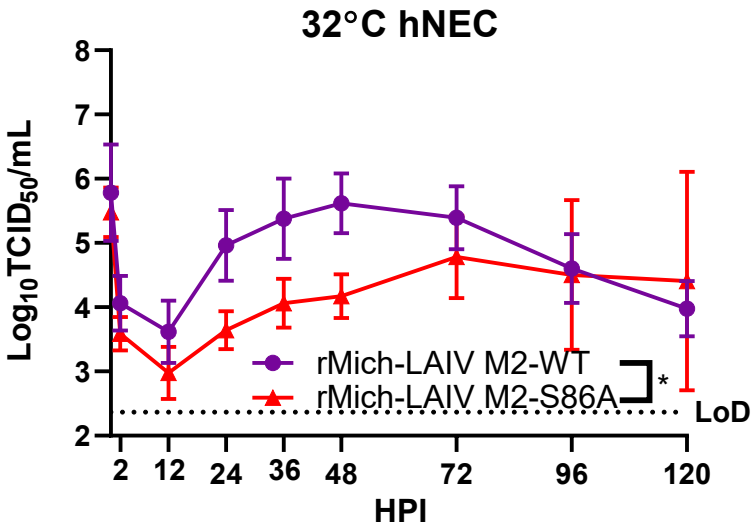

Fig. 7- 32°C H1N1 hNEC GC. A multi-step growth curve was performed on hNEC cells with the indicated H1N1 recombinant viruses at 32°C with an MOI 0.1. Statistical significance was measured with a two-way ANOVA followed by Bonferroni post-test. Results are from 3 independent experiments, each with 4 technical replicates. *p<0.05.

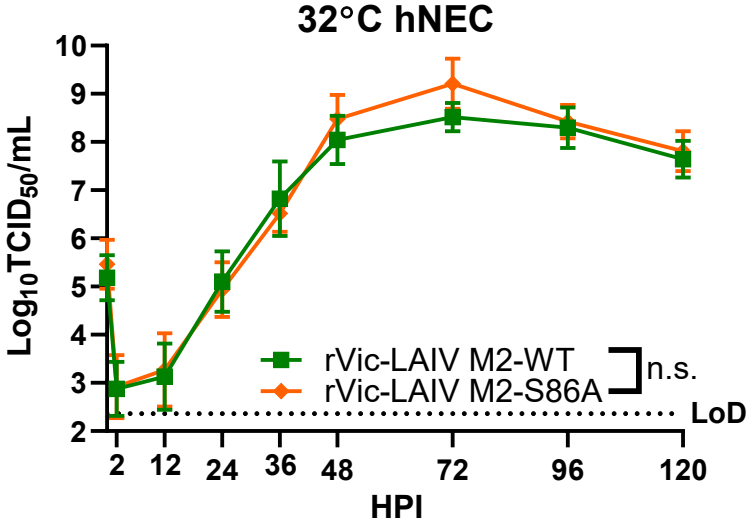

Fig. 8- 32°C H3N2 hNEC GC. A multi-step growth curve was performed on MDCK cells with the indicated H3N2 recombinant viruses at 32°C with an MOI 0.1. Statistical significance was measured with a two-way ANOVA followed by Bonferroni post-test. Results are from 3 independent experiments, each with 4 technical replicates. *p<0.05.

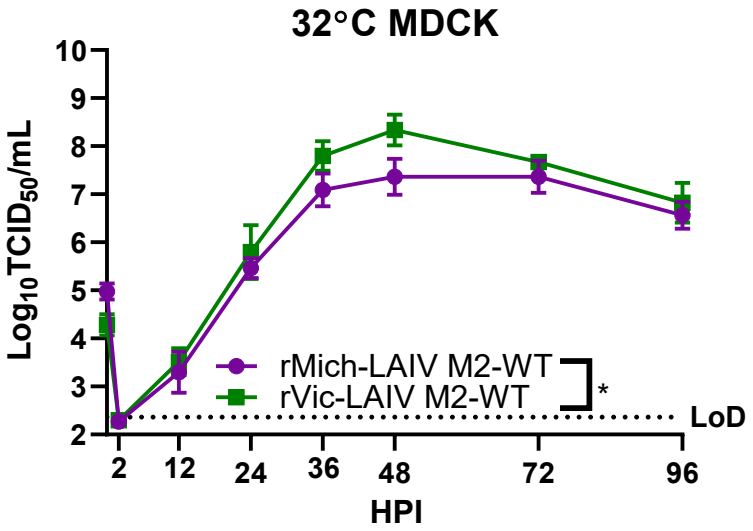

Fig. 10- 32°C H1N1vH3N2 MDCK GC. A multi-step growth curve was performed on MDCK cells with the M2-WT H1N1 and H3N2 recombinant viruses at 32°C with an MOI 0.01. Statistical significance was measured with a two-way ANOVA followed by Bonferroni post-test. Results are from 3 independent experiments, each with 4 technical replicates. *p<0.05.MOI 0.01, Two-way ANOVA, n=3, 4 tech. reps

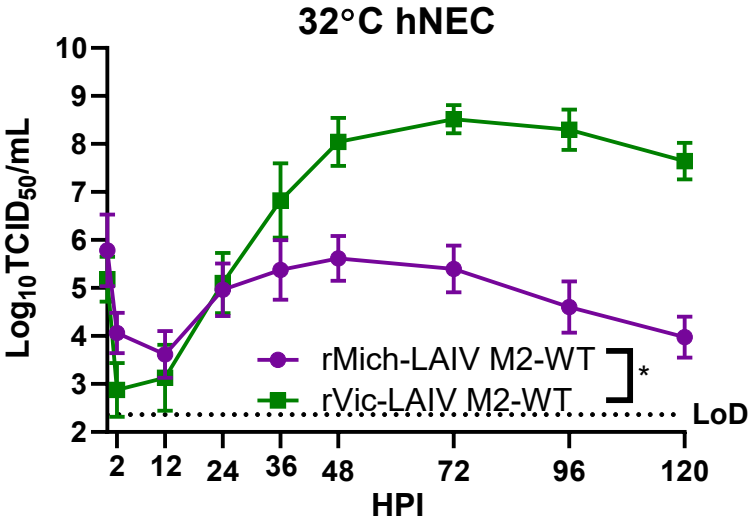

Fig. 9- 32°C H1N1vH3N2 hNEC GC. A multi-step growth curve was performed on hNEC cells with the M2-WT H1N1 and H3N2 recombinant viruses at 32°C with an MOI 0.1. Statistical significance was measured with a two-way ANOVA followed by Bonferroni post-test. Results are from 3 independent experiments, each with 4 technical replicates. *p<0.05.MOI 0.01, Two-way ANOVA, n=3, 4 tech. reps

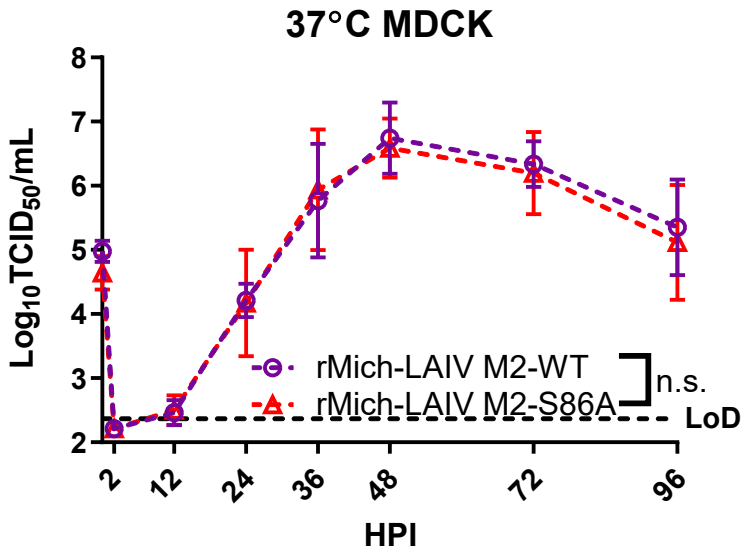

Fig. 11- 37°C H1N1 MDCK GC. A multi-step growth curve was performed on MDCK cells with the indicated H1N1 recombinant viruses at 37°C with an MOI 0.01. Statistical significance was measured with a two-way ANOVA followed by Bonferroni post-test. Results are from 3 independent experiments, each with 4 technical replicates. *p<0.05.

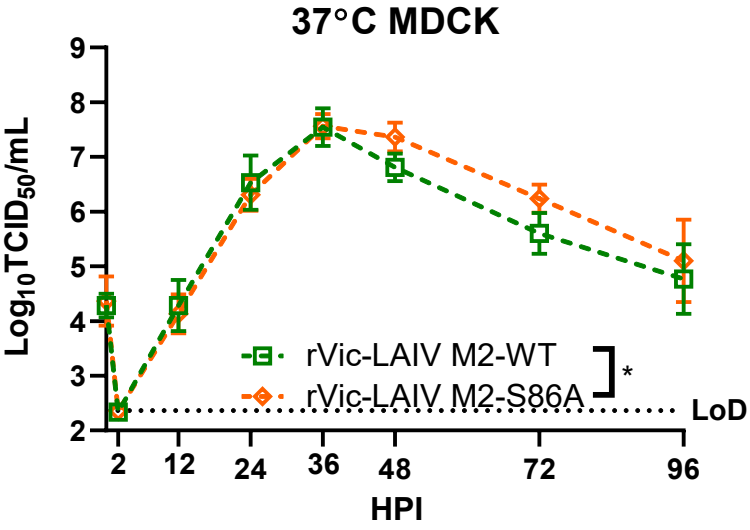

Fig. 12- 37°C H3N2 MDCK GC. A multi-step growth curve was performed on MDCK cells with the indicated H3N2 recombinant viruses at 32°C with an MOI 0.01. Statistical significance was measured with a two-way ANOVA followed by Bonferroni post-test. Results are from 3 independent experiments, each with 4 technical replicates. *p<0.05.

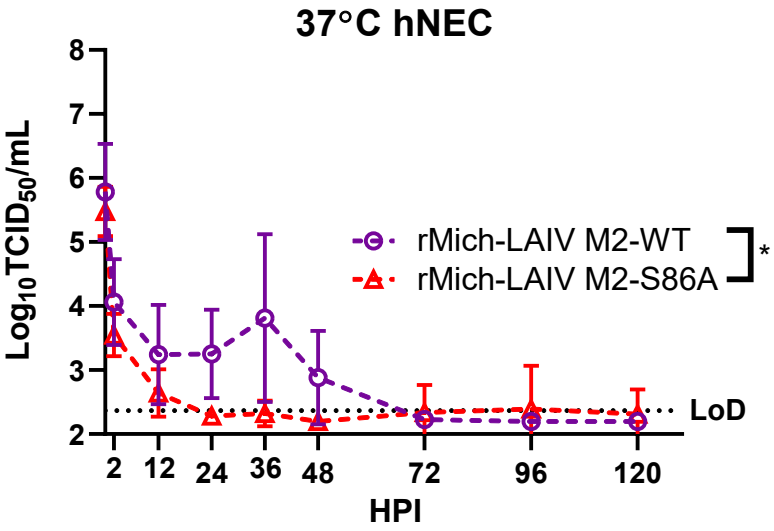

Fig. 13- 37°C H1N1 hNEC GC. A multi-step growth curve was performed on hNEC cells with the indicated H1N1 recombinant viruses at 37°C with an MOI 0.1. Statistical significance was measured with a two-way ANOVA followed by Bonferroni post-test. Results are from 3 independent experiments, each with 4 technical replicates. *p<0.05.

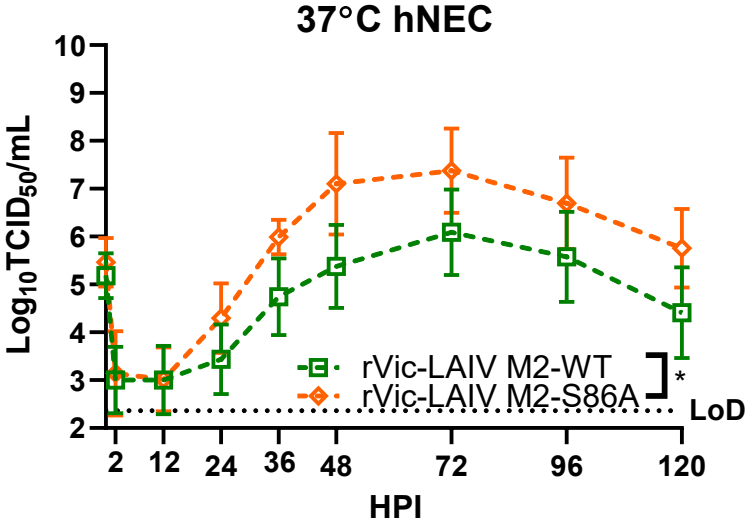

Fig. 14- 37°C H3N2 hNEC GC. A multi-step growth curve was performed on hNEC cells with the indicated H3N2 recombinant viruses at 37°C with an MOI 0.1. Statistical significance was measured with a two-way ANOVA followed by Bonferroni post-test. Results are from 3 independent experiments, each with 4 technical replicates. *p<0.05.

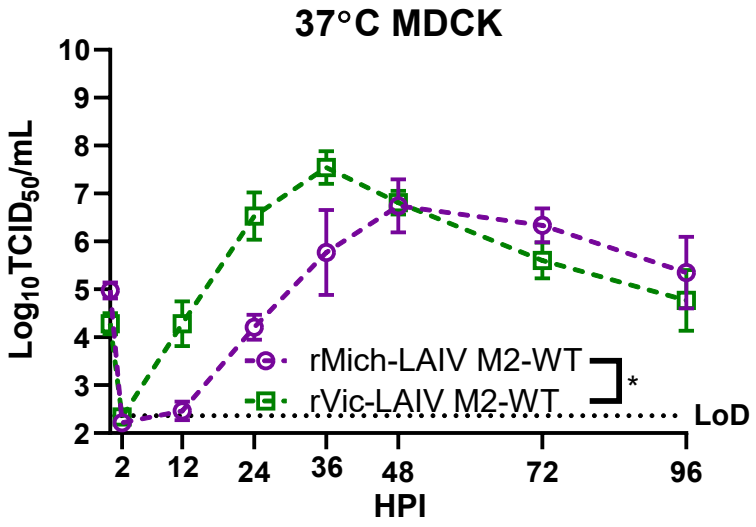

Fig. 16- 37°C H1N1vH3N2 MDCK GC. A multi-step growth curve was performed on MDCK cells with the M2-WT H1N1 and H3N2 recombinant viruses at 37°C with an MOI 0.01. Statistical significance was measured with a two-way ANOVA followed by Bonferroni post-test. Results are from 3 independent experiments, each with 4 technical replicates. *p<0.05.MOI 0.01, Two-way ANOVA, n=3, 4 tech. reps

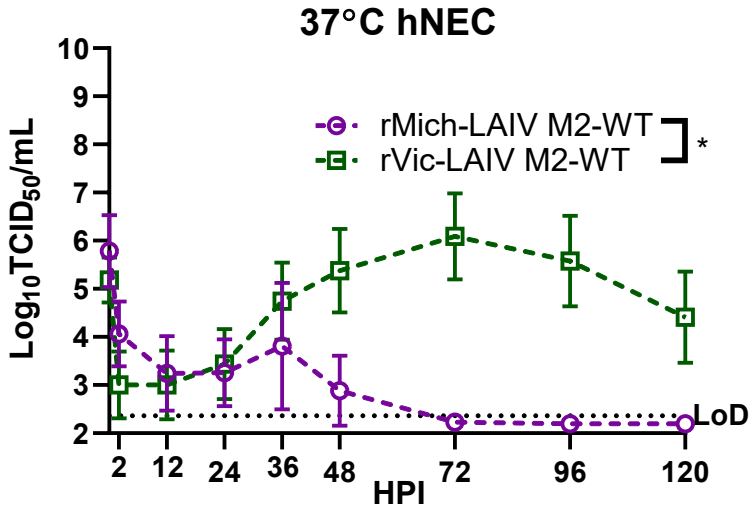

Fig. 15- 37°C H1N1vH3N2 hNEC GC. A multi-step growth curve was performed on hNEC cells with the M2-WT H1N1 and H3N2 recombinant viruses at 37°C with an MOI 0.1. Statistical significance was measured with a two-way ANOVA followed by Bonferroni post-test. Results are from 3 independent experiments, each with 4 technical replicates. *p<0.05.MOI 0.01, Two-way ANOVA, n=3, 4 tech. reps

Chapter 3: CHARACTERIZATION OF H1 VARIANT VIRUSES

BACKGROUND

HA is one of influenza virus's two surface proteins and is responsible for receptor binding, typically to α2,6-linked sialic acids found predominantly in the human upper respiratory tract, and membrane fusion [27]. The most recent, notable HA change came during the 2009 H1N1 pandemic, where a swine-based HA protein garnered enough mutations to become pathogenic in the human population. Subsequent analysis of the new HA found several mutations that increase the virus's thermal stability, lower the required pH for fusion, and increased the acidic stability [31]. With this global change in the circulating H1N1 virus, updates to seasonal vaccines were necessary to confer protection. FluMist used the surface protein from the virus being used in the IIV, A/California/7/2009. The A/Cal/7/2009 LAIV appeared effective in the low H1N1 seasons following 2009, however, when a predominantly H1N1 season occurred in 2013, it revealed that the H1N1 component of FluMist was highly ineffective, while the IIV showed effectiveness around 60%. This led the manufacturer to change the surface proteins being used for the 2015-2016 season to A/Bolivia/55/2013. Despite the change, the H1N1 component of FluMist was still providing no protection against circulating H1N1 viruses. This led the ACIP to pull FluMist off the US market to prevent another season of poor vaccine efficacy. During its time off the market, the manufacturer has since changed the surface proteins to A/Slovenia/2903/2015. The new surface proteins have displayed increased replication in nasal epithelial cell cultures and increased capability to survive multiple rounds of replication [43].

Given this information along with reviewing the data from our recombinant viruses' inability to survive and replicate on hNEC cultures, this has led us to try different surface proteins, including a pre-2009 H1N1 (A/New Caledonia/20/99), the A/Bolivia HA which was in the vaccine when FluMist was pulled off of the market, and A/Slovenia that is currently in the licensed vaccine, with our M2 mutation. This panel of H1 surface proteins should elicit how well these recombinant viruses can replicate on a physiologically relevant model and what, if any, affect our M2 mutation has on H1 viruses.

MATERIALS AND METHODS

PLASMIDS

Plasmids encoding A/Slovenia and A/Bolivia were designed based on available sequences, put into pHH21, and purchased through GenScript (GenScript USA Inc., Piscataway, NJ). A plasmid encoding a pre-2009 H1 HA, A/New Caledonia/20/99, is currently being generated through GenScript's services.

The internal plasmid of pHH21 M LAIV encodes the entire influenza H2N2 A/Ann Arbor/6/60 M segment under control of the human RNA polymerase I promotor and murine RNA polymerase I terminator [50]. Mutations were introduced to the plasmid using the QuikChange Lightning site-directed mutagenesis (Agilent, Santa Clara, CA) protocol. The sequences of the forward and reverse mutagenesis primers used to introduce the S86A mutation are in Table 1 (M2_S86A_1 and M2_S86A_2).

Using Dpn1 enzyme for digestion, the parental DNA was removed from the PCR product, and the product was transformed into competent bacterial (DH5α) cells. DNA from multiple bacterial clones was extracted using QIAprep Spin Miniprep Kit (Qiagen). Using an LAIV M segment-specific primer, H2N2 LAIV Mseq 660F (Table 1), the DNA was sequenced for the appropriate mutations.

CELL LINES

Madin Darby canine kidney (MDCK) and human embryonic kidney 293T (293T) cells were cultured in Dulbecco's Modified Eagle Medium (DMEM, Sigma-Aldrich) with 10% fetal bovine serum (FBS, Gibco Life Technologies), 100U penicillin/mL with 100μg streptomycin/mL (Quality Biological), and 2mM L-Glutamine (Gibco Life Technologies) at 37°C with air supplemented with 5% CO_2.

Human nasal epithelial cell (hNEC) cultures will be isolated from non-diseased tissue after endoscopic sinus surgery for non-infection related conditions [25]. The cells will be differentiated at an air-liquid interface (ALI) in 24-well Falcon filter inserts (0.4-μM pore; 0.33cm^2; Becton Dickinson) before infection, using ALI medium as basolateral medium.

REVERSE GENETICS

Recombinant viruses were rescued using a 12 plasmid reverse genetics system [50]. All eight segments of the target virus are required, in addition to helper plasmids encoding viral replication machinery. 293T cells were infected with 0.5μg of pHH21 plasmids encoding A/Ann Arbor/6/60 LAIV internal genes PB2, PB1, PA, NP, NS, and the WT and M2-S86A mutant M. 0.5μg of A/Bolivia/55/2013 or A/Slovenia/2903/2015 HA and A/Michigan/45/2015 NA in the pHH21 plasmid were added to supply the surface proteins Additionally, 1μg of protein expression plasmids for A/Udorn/72 PB2, PB1, and NP plus 0.2μg PA were added as plasmids that would reconstitute the influenza polymerase activity. When the 8 target virus plasmids infect the 293T cells, their corresponding vRNA is produced but unable to be replicated. The polymerase-containing replication machinery in the helper plasmids allow the vRNA to be replicated to produce more infectious virus particles.

TransIT-LT-1 (LT1) (Mirus, Madison, WI), a transfection reagent, was mixed with OptiMEM medium (Gibco, Carlsbad, CA) and incubated at room temperature for 15 minutes at a ratio of 2uL LT1 to 1ug plasmid DNA. The 12 plasmids were added to the solution and incubated at room temperature for 15 minutes. Complete medium was removed from 293T cells in 6-well plates and replaced with 2mL OptiMEM. The LT1-

OptiMEM-plasmid solutions were then added to each well. The plates were incubated at 32°C with 5% CO_2 for 24 hours. N-acetyl trypsin (NAT) (Sigma, St. Louis, MO) was added to a final concentration of 10ug/ml to each well, and the plates were incubated for another 4 hours at 32°C with 5% CO_2. $5x10^5$ MDCK cells in 100uL infection medium were added to each well, and the plate was incubated at 32°C with 5% CO_2. 1mL of transfected cell supernatant was collected and replaced with 1mL DMEM with 4ug/ml NAT, 100u/ml penicillin 100ug/ml streptomycin, 2mM L-Glutamine and 0.5% bovine serum albumin (BSA) (Sigma) (infectious medium with NAT, IM+NAT) daily until obvious signs of cytopathic effect were visible.

SEQUENCING

After plasmid, seed stock, and working stock generation, Sanger sequencing was utilized to confirm the appropriate M2-86 amino acid and HA was in each virus. The sequencing was done at the Synthesis & Sequencing Facility of the Johns Hopkins University (Baltimore, MD) using Applied Biosystems 3730xl DNA Analyzer and dye terminator sequencing technology. DNA plasmid concentration was found using the NanoDrop spectrophotometer ND-1000 (Thermo Fisher Scientific). The primer H2N2 LAIV Mseq 660F (Table 1) was used to confirm the M protein sequence, while pHH21-1 F and pHH21-2 R (Table 1: Primer Sequences) were used to confirm the HA proteins.

SEED STOCKS AND WORKING STOCKS

To generate seed stocks, fully confluent 6-well plates of MDCK cells were washed 2 times with PBS+ and then infected with 250µL of the plaque pick solution for 1 hour, with redistribution every 15 minutes, at 32°C with 5% CO_2. After 1 hour, the infection media was removed and 2mL of IM+NAT (1:1000) was added. Virus supernatant was

collected with 75% of the cells showed cytopathic effect, typically 5 days post-infection. The seed stocks were titrated via $TCID_{50}$ assay. Working stocks were generated from seed stocks, in a similar fashion, except on fully confluent MDCK cells in $75cm^2$ flasks, and the seed stock inoculum was diluted to an MOI of 0.001 in IM.

PLAQUE ASSAY

Plaque assays are being performed in 90-100% confluent 6-well plates of MDCK cells. 250µL of serial 10-fold dilutions of transfection supernatant in IM+NAT (1:1000) were added to each well, and incubated at 32°C, for plaque picking or plaque morphology studies, or 37°C, for plaque morphology only, with 5% CO_2 for one hour, with gentle distribution of the solution every 15 minutes. Wells were then covered with 2% agarose combined with 2X MEM plus 1:1000 NAT. Once the agarose solidified, plates were incubated at 32°C, for plaque picking or plaque morphology studies, or 37°C, for plaque morphology only, with 5% CO_2 for 5 days. After 5 days, one of two protocols was followed. Plaques could be picked using a 1mL blunt pipette tip, added to tubes containing IM, and stored at -80°C to be used to establish seed stocks of the virus colony. Alternatively, plates could be fixed with 4% formaldehyde in PBS overnight and stained with Napthol Blue Black overnight to be used to quantify plaque size and morphology.

To quantify plaque area, images of the wells will be captured using a dissecting microscope with an Olympus DP-70 color camera. A standard ruler image was also taken to set a reference. Photos were opened in ImageJ (NIH), a reference length of 1cm was measured via the ruler image, and borders were drawn around individual plaques using the Freehand selector. Measurements of the area of the plaque will be calculated in

ImageJ, and data was graphed and analyzed in GraphPad Prism 8 (GraphPad Software, San Diego, CA).

$TCID_{50}$ ASSAY

Fifty percent tissue culture dose ($TCID_{50}$) was determined in 96-well plates of 90-100% confluent MDCK cells. After being washed twice with PBS+, ten-fold serial dilutions of the viruses in IM+NAT (1:1000) were made, and 20µL of each dilution was added to 6 wells. The plates were incubated at 32°C with 5% CO_2 for 7 days. The cells were fixed with 4% formaldehyde (Fisher Chemical) in PBS for at least 1 hour and then stained with Napthol Blue Black solution overnight. Endpoint values were calculated by the Reed-Muench method [51].

LOW MULTIPLICITY OF INFECTION (MOI) GROWTH CURVES (GC)

Low MOI GCs are being used to determine viral growth kinetics. The low MOI promoted multiple rounds of virus replication, thereby optimizing the detection of replication differences between virus strains. An MOI of 0.01 is used in MDCK cells and 0.1 in hNECs. For MDCK cell infections, 100% confluent 24-well plates of MDCK cells are washed 3 times with PBS+. The virus inoculum is diluted in IM, 100µL is added to the cells, and allowed to incubate at 32°C or 37°C for 1 hour, with redistribution every 15 minutes. The inoculum is removed, the cells are washed 3 times with PBS+ and incubate with 500µL of IM+NAT (1:1500). At the indicated times, all media is collected and fresh IM+NAT was re-supplemented.

For hNEC cell infections, fully differentiated 24-well plates with a transwell membrane will have their basolateral media replaced and will be washed 3 times on the apical side with IM, with a10 minute 32°C or 37°C with 5% CO_2 incubation between

each wash. The virus inoculum will be diluted in IM, 100 µL will be added to the cells, and allowed to incubate at 32°C or 37°C for 2 hours. The inoculum is removed, the cells are washed 3 times with PBS+ and incubate at 32°C or 37°C with 5% CO_2. At the indicated times, IM will be added to the apical side, allowed to incubate at the corresponding temperature for 10 minutes, and then collected. Basolateral media will be collected and replaced every 48 hours. Infectious virus particle production was quantified using a $TCID_{50}$ on MDCK cells.

RESULTS

Rescue of recombinant influenza viruses encoding M2-S86A mutations

The A/Ann Arbor/6/1960 (H2N2) LAIV M2 protein contains an Alanine to Serine mutation at position 86 of the M2 cytoplasmic tail, which was acquired during the cold adaptation process of the virus [52]. Recombinant H1N1 viruses expressing A/Bolivia/55/2013 and A/Slovenia/2903/2015 HA with either LAIV M2-WT or LAIV M2-S86A were successfully generated. The entire coding region of the M segment of each virus was sequenced to confirm the expression of the desired mutation and to verify no other amino acid mutations were present. The HA segments were also sequence verified.

Replication of recombinant viruses at 32°C

To evaluate the viruses' abilities to survive multiple rounds of replication and spread cell to cell, multistep low MOI growth curves of both viruses were performed on MDCK cells and differentiated hNECs at 32°C to replicate the temperature of the upper portion of the human respiratory tract.

On MDCK cells, rSlov-LAIV M2-WT and rBol-LAIV M2-S86A both reached peak infectious virus titer at 36 hours post infection, while rBol-LAIV M2-WT and rSlov-LAIV M2-WT reached it at 48 hours post infection (Fig. 17). rSlov-LAIV M2-S86A reached the highest peak titer and rSlov-LAIV M2-WT reached the lowest highest titer, but this difference is less than 5-fold and not considered biologically relevant. rBol-LAIV M2-WT took longer and lower titers leading up to reach its peak viral titer than rSlov-LAIV M2-WT but sustained a higher titer after 48 hours than rSlov-LAIV M2-WT, and this difference was found to be statistically significant. Similarly, rBol-LAIV M2-

S86A reached a lower peak titer faster, with higher titers leading up to its peak titer, than rSlov-LAIV M2-S86A, but rSlov-LAIV M2-S86A sustained a higher viral titer after its peak titer, and these differences were found to be statistically significant. These data suggest that there is some biologically relevant difference between the initial kinetics based on the HA and M proteins used, but the ultimate viral titer is not affected by these proteins on immortalized cells.

Replication of recombinant viruses at 37°C

In addition to growth curves at 32°C, low MOI growth curves were performed on MDCK cells at 37°C. The lower portion of the human respiratory tract and core human body temperature sits around 37°C, and growth curves at this temperature would elucidate any potential temperature sensitivity this mutation is responsible for.

On MDCK cells, all viruses except rSlov-LAIV M2-WT reached a peak viral titer at 48 hours post infection, while rSlov-LAIV M2-WT reached its peak titer at 24 hours post infection (Fig. 18). rBol-LAIV M2-WT and rSlov-LAIV M2-S86A replicated with similar kinetics both before and after they reached their peak viral titers and reached similar levels of peak titers. Meanwhile, rSlov-LAIV M2-WT and rBol-LAIV M2-S86A replicated with higher kinetics before reaching their peak viral titers, and rBol-LAIV M2-S86A reached a similar peak titer as rBol-LAIV M2-WT and rSlov-LAIV M2-S86A. Given the up to 3-log growth difference in kinetics before and 1.5-log difference in viral titer after 48 hours post infection, there was a statistically significant difference between rSlov-LAIV M2-WT and rBol-LAIV M2-WT. Meanwhile, rBol-LAIV M2-S86A grew to higher titers in the first half of the assay, but rSlov-LAIV M2-S86A had a higher peak viral titer and maintained a higher titer in the second half of the assay. These differences

did not display a statistical significance. Despite occurring on immortalized cells, this assay could be hinting at the effect of the higher temperature on replication between these viruses.

Replication of similar recombinant viruses at different temperatures

As for each virus compared to its temperature different assay, on MDCK cells, rSlov-LAIV M2-WT and rSlov-LAIV M2-S86A reached and maintained higher titers at 32°C than 37°C, which is expected due to the temperature sensitive phenotype of the LAIV virus (Fig. 19). This ensures that our temperature sensitive phenotype was held within the recombinant viruses. rSlov-LAIV M2-WT reached peak titers at 36 hours post infection for both temperatures, while rSlov-LAIV M2-S86A reached peak viral titer at 48 hours post infection at both temperatures. The difference between the peak titers for rSlov-LAIV M2-WT was less than 4-fold, which is quite different from the 7-fold, and more biologically relevant, difference of rSlov-LAIV M2-S86A. While the difference between the kinetics of rSlov-LAIV M2-WT and rSlov-LAIV M2-S86A at 32°C was not found to be statistically significant, the differences before and after peak viral titer were reached at 37°C was statistically significant. Given the higher peak viral titers and sustained titers after, at both 32°C and 37°C, rSlov-LAIV M2-S86A may be more fit than rSlov-LAIV M2-WT.

For the recombinant A/Bolivia viruses, both rBol-LAIV M2-WT and rBol-LAIV M2-S86A had faster kinetics and higher titers at 32°C than 37°C, which is to be expected (Fig. 20). A 10-fold difference was seen between each respective virus at both temperatures. rBol-LAIV M2-S86A was the only recombinant Bolivia virus to reach a peak viral titer at 36 hours post infection, while the other 3 viruses peaked at 48 hours

post infection. Given the more than 10-fold difference between the kinetics of rBol-LAIV M2-WT and rBol-LAIV M2-S86A, a statistically significant difference was seen at 32°C. Despite the difference in the early kinetics of both viruses at 37°C, the peak titer and subsequent kinetics did not show a statistical significance. Unlike the recombinant Slovenia viruses, the differences between rBol-LAIV M2-WT and rBol-LAIV M2-S86A do not appear to be as dramatic between the M2 variants.

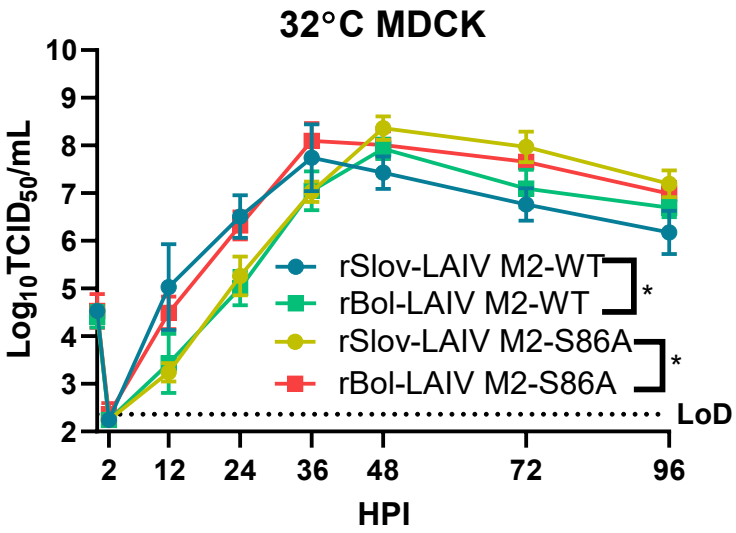

Fig. 17- 32°C H1 panel MDCK GC. A multi-step growth curve was performed on MDCK cells with the indicated H1N1 recombinant viruses at 32°C with an MOI 0.01. Statistical significance was measured with a two-way ANOVA followed by Bonferroni post-test. Results are from 2 independent experiments, each with 4 technical replicates. *p<0.05.

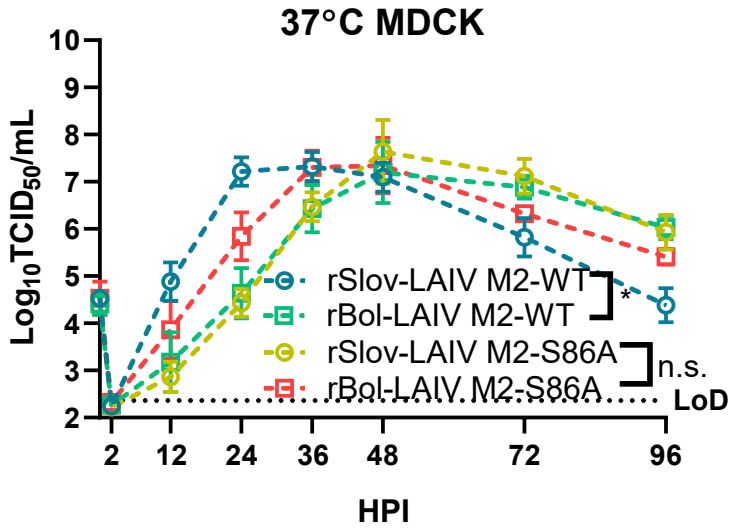

Fig. 18- 37°C H1 panel MDCK GC. A multi-step growth curve was performed on MDCK cells with the indicated H1N1 recombinant viruses at 37°C with an MOI 0.01. Statistical significance was measured with a two-way ANOVA followed by Bonferroni post-test. Results are from 2 independent experiments, each with 4 technical replicates. *p<0.05.

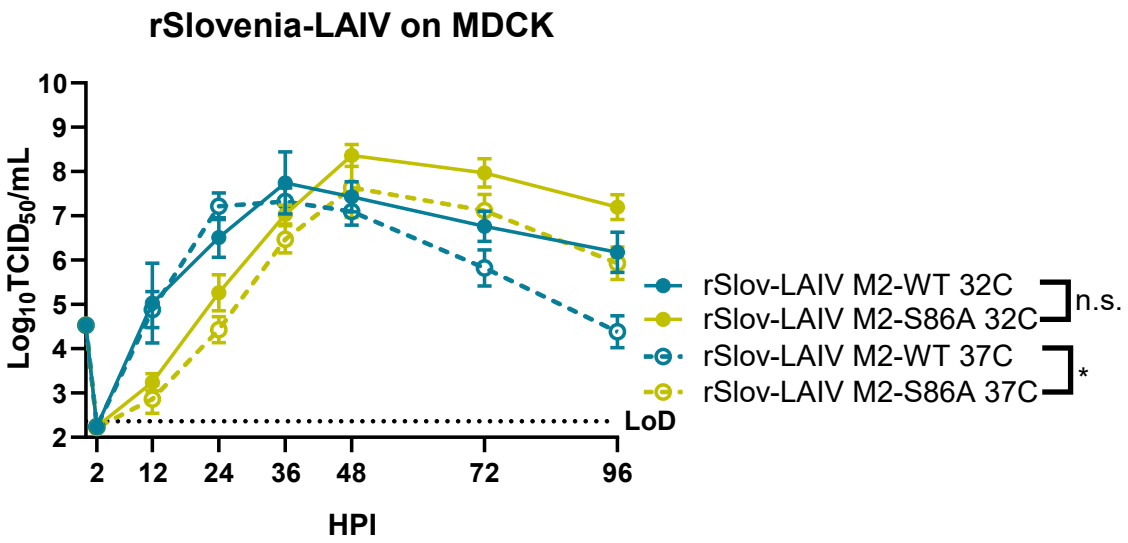

Fig. 20- 32°C and 37°C rSlovenia MDCK GC. A multi-step growth curve was performed on MDCK cells with the indicated H1N1 recombinant viruses at 32°C and 37°C with an MOI 0.01. Statistical significance was measured with a two-way ANOVA followed by Bonferroni post-test. Results are from 2 independent experiments, each with 4 technical replicates. *p<0.05.

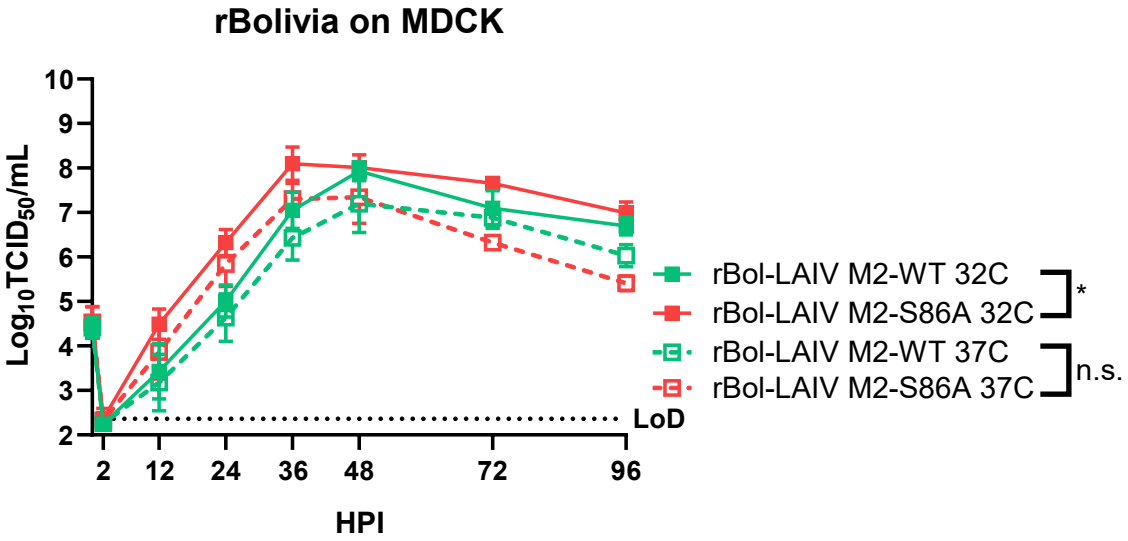

Fig. 19- 32°C and 37°C rBolivia MDCK GC. A multi-step growth curve was performed on MDCK cells with the indicated H1N1 recombinant viruses at 32°C and 37°C with an MOI 0.01. Statistical significance was measured with a two-way ANOVA followed by Bonferroni post-test. Results are from 2 independent experiments, each with 4 technical replicates. *p<0.05.

DISCUSSION

CHARACTERIZATION OF M2 MUTATED VIRUSES

The cytoplasmic tail of the LAIV M protein has been mapped to have roles in genome packaging and virus attenuation [25]. Disruption in this tail led to a defect in infectious virus particle production, and specifically the amino acid in the 86th position may have a significant role in this phenotype. After finding that the only difference between the WT and cold-adapted strains of the master donor virus for LAIV viruses, A/Ann Arbor/6/1960, was a mutation at M2 position 86, recombinant H3N2 viruses with both amino acids were generated. After studying the viruses' kinetics on immortalized and physiologically-relevant models, the LAIV M2-WT amino acid was found to increase replication in hNEC cultures at 37°C, which was associated with an altered induction of IFN-λ production. This study aimed to characterize this mutation on an H1N1 backbone. Aside from further characterizing influenza virus, these results were relevant for LAIV virus study because FluMist was removed from the US market for the 2016/2017 and 2017/2018 seasons due to a faulty H1N1 component. An increase in viral replication could show an easy mutation to introduce into the virus being used in the vaccine and increase vaccine efficacy.

However, the data presented here show that while the LAIV M2-WT amino acid had increased replication over the M2-S86A mutation, these differences are hard to interpret on hNECs since H1N1 viruses performed significantly worse than their H3N2 counterparts, with rMich-LAIV M2-S86A failing to replicate at 37°C (Fig. 13). These results are also opposite of the effects seen with this mutation on an H3N2 LAIV virus. Despite the virus's poor replication capability on hNEC cultures, the mutation appears to

play no role in the virus's ability to replicate on an immortalized cell line (Fig. 10, Fig. 11). This phenotype has been characterize before and emphasizes the need to use physiologically relevant models and temperatures when working with LAIV viruses [53].

CHARACTERIZATION OF H1 VARIANT VIRUSES

The lack of studying the LAIV viruses on a human physiologically relevant cell culture models led to the poor selection of the H1N1 component of FluMist starting in 2013. After several years of a decreased effectiveness and the vaccine being pulled off the US market, studies found that the failing H1N1 component was unable to replicate on human cells [46]. Previous assays to assess the candidate viruses only determined how well the virus was able to bind to and infect an immortalized cell line. When the new candidate virus was selected for the 2018/2019 season, it demonstrated the ability to not only to bind to and infect immortalized cells, but to infect and replicate on hNEC cultures as well. When the virus used in the vaccine in 2014/2015, that was ultimately removed from the market, was assessed under these new conditions, it was found that it failed to replicate on human cells, a pivotal component of a successful LAIV virus. After seeing a similar phenotype in the surface proteins used in our studies, we decided to test our M2-86 mutation using the surface proteins from before the 2009 pandemic that caused the reformulation of FluMist, from the failed vaccine virus, and from the approved vaccine virus.

Studies using the HA protein from 2015 and 2018 are in their preliminary stages. Plaque assays to assess the morphology at both 32°C and 37°C are currently being conducted and imaged to quantify plaque size. The first replicate of a low MOI hNEC growth curve is being run at both 32°C and 37°C. Two replicates of low MOI MDCK cell

growth curves have been completed. Thus far, all four viruses have shown they maintain their temperature sensitives between 32°C and 37°C. Given the statistically significant, but not necessarily biologically relevant difference between rSlov-LAIV M2-WT and rBol-LAIV M2-WT, it is no surprise that rBol-LAIV M2-WT looked to be an effective vaccine virus when grown on immortalized cells. Similarly, while both M2-S86A mutants reach higher peak viral titers faster than their M2-WT counterpart, the true effect of this mutation, and the role the HA protein plays, will be more relevant when looked at on hNEC cultures.

FUTURE DIRECTIONS

As previously stated, the pre-2009 HA from A/New Caledonia/ 20/1999 is currently being generated. Upon receiving, the M2-WT and M2-S86A plasmids will be used to recuse the viruses and generate seed and working stocks. These new viruses, along with the four currently generated will be put through the "trinity" of experiments previously described in Chapter 2 – plaque size on MDCK cells, low MOI growth curves in MDCK and hNEC cultures. The rBolivia-LAIV M2-WT and M2-S86A and rSlovenia-LAIV M2-WT and M2-S86A have working stocks which have been titered and verified, with early experiments underway. These experiments will demonstrate how well the individual viruses are able to infect neighboring cells, replicate on immortalized cells, and infect and replicate hNEC cultures. Once these experiments are complete, we can evaluate how these surface proteins factor into a virus's ability to infect and replicate, and how well these different viruses can tolerate the M2-86 mutation. Ultimately, this will give us a glimpse into how this M2 mutation may or may not have an attenuation role. The use of primary epithelial cell cultures and the understanding that not all HA and NA proteins are created equal when it comes to replication in primary epithelial cell cultures has improved our understanding of how to characterize new LAIV viruses in order to ensure that they are replicating efficiently, and therefore have a good chance at being an effective influenza vaccine.

ELISA interferon, cytokine, and chemokine panels can elucidate how the immunologic response is different in hNEC cultures between the viruses and how viruses that generate more infectious virus particles may be eliciting a different response than viruses generating less infectious particles. Flow cytometry can be utilized to analyze

how efficient the viruses are at infected uninfected cells and if there is a difference in efficiency between viruses that are able to generate more infectious virus particles. These experiments could also provide insights into how LAIV strains may be modulating their replication and induced innate immune responses, perhaps also shedding light on how these factors might affect LAIV vaccine efficacy.

Label	Purpose	Sequence
M2_S86A_1	SDM	5’- AAA ATG ACT ATC GTC AGC ATC CAC AGC ACT CTG CTG -3’
M2_S86A_2	SDM	5’- CAG CAG AGT GCT GTG GAT GCT GAC GAT AGT CAT TTT -3’
H2N2 LAIV Mseq 660F	M segment sequence confirmation	5’- GAC TCA TCC TAG CTC CAG TGC TG -3’
pHH21_1	HA segment sequence confirmation	5’- GGT ATA TCT TTC GCT CCG AG -3’
pHH21 seq2 (rev)	HA segment sequence confirmation	5’- CAC TTT CGG ACA TCT GGT -3’
LAIV M S86V For tm 65.9	SDM	5’- CAA AAT GAC TAT CGT CAA CAT CCA CAG CAC TCT GCT GTT CCT -3’
LAIV M S86S Rev tm 65.9	SDM	5’- AGG AAC AGC AGA GTG CTG TGG ATG TTG ACG ATA GTC ATT TTG -3’
New Caledonia HA 5’ UTR	New Caledonia RTPCR primer	5’- AAA GCA GGG GAA AAC AAA AGC AAC AAA AAA TGA AAG CAA AAC TAC TGG -3’
New Caledonia HA 3’ UTR	New Caledonia RTPCR primer	5’- GAA ACA AGG GTG TTT TTC TCA TGA TTC TGA AAT CCT AAT GTC AGA TGC ATA TTC T -3’

Table 1: Primer Sequences

BIBLIOGRAPHY

1. **About Flu** [https://www.cdc.gov/flu/about/index.html]
2. **Influenza (Flu) Viruses** [https://www.cdc.gov/flu/about/viruses/index.htm]
3. **Influenza (Flu)** [https://www.cdc.gov/flu/about/disease/spread.htm]
4. **Seasonal Flu vs. Pandemic Flu** [https://www.cdc.gov/flu/resource-center/freeresources/graphics/seasonal-vs-pandemic-flu-infographic.htm]
5. Reid AH, Taubengerger JK, Fanning TG: **Evidence of an absence: the genetic origins of the 1918 pandemic influenza virus**. *Nature Reviews Microbiology* 2004, **2**:909-914.
6. **Remembering the 1918 Influenza Pandemic** [https://www.cdc.gov/features/1918-flu-pandemic/index.html]
7. Swerdlow DL, Finelli L, Bridges CB: **2009 H1N1 Influenza Pandemic: Field and Epidemiologic Investigations in the United States at the Start of the First Pandemic of the 21st Century**. *Clinical Infectious Diseases* 2011, **52**:S1-S3.
8. Jhung MA, Swerdlow D, Olsen SJ, Jernigan D, Biggerstaff M, Kamimoto L, Kniss K, Reed C, Fry A, Brammer L *et al*: **Epidemiology of 2009 Pandemic Influenza A (H1N1) in the United States**. *Clinical Infectious Diseases* 2011, **52**:S13-S26.
9. Mena I, Nelson ML, Quezada-Monroy F, Dutta J, Cortes-Fernandez R, Lara-Puente JH, Castro-Peralta F, Cunha LF, Trovao NS, Lozano-Dubernard B *et al*: **Origins of the 2009 H1N1 influenza pandemic in swine in Mexico**. *eLife* 2016, **5**:e16777.
10. **H1N1 Flu** [https://www.cdc.gov/h1n1flu/cdcresponse.htm]
11. **Past Pandemics** [https://www.cdc.gov/flu/pandemic-resources/basics/past-pandemics.html]
12. Shrestha SS, Swerdlow DL, Borse RH, Prabhu VS, Finelli L, Atkins CY, Owusu-Edusi K, Bell B, Mead PS, Biggerstaff M *et al*: **Estimating the Burden of 2009 Pandemic Influenza A (H1N1) in the United States (April 2009–April 2010)**. *Clinical Infectious Diseases* 2011, **52**(suppl_1):S75–S82.
13. **Types of Influenza Viruses** [https://www.cdc.gov/flu/about/viruses/types.htm]
14. Bouvier NM, Palese P: **The biology of influenza viruses**. *Vaccine* 2008, **26**:D49-D53.
15. **Overview of Influenza Surveillance in the United States** [https://www.cdc.gov/flu/weekly/overview.htm]
16. **Estimated Influenza Illnesses, Medical visits, Hospitalizations, and Deaths in the United States — 2017–2018 influenza season** [https://www.cdc.gov/flu/about/burden/estimates.htm]
17. Biggerstaff M, Jhung M, Kamimoto L, Balluz L, Finelli L: **Self-Reported Influenza-Like Illness and Receipt of Influenza Antiviral Drugs During the 2009 Pandemic, United States, 2009–2010**. *American Journal of Public Health* 2012, **102**(10):e12-e26.
18. **Disease Burden of Influenza** [https://www.cdc.gov/flu/about/burden/index.html]
19. Molinari N-AM, Ortega-Sanchez IR, Messonnier ML, Thompson WW, Wortley PM, Weintraub E, Bridges CB: **The annual impact of seasonal influenza in the US: Measuring disease burden and costs**. *Vaccine* 2007, **25**:5086=5096.

20. **How the Flu Virus Can Change: "Drift" and "Shift"** [https://www.cdc.gov/flu/about/viruses/change.htm]
21. Brooke CB, Ince WL, Wrammert J, Ahmed R, Wilson PC, Bennink JR, Yewdell JW: **Most Influenza A Virions Fail To Express at Least One Essential Viral Protein**. *Journal of Virology* 2013, **87**(6):3155-3162.
22. Saira K, Lin X, DePasse JV, Halpin R, Twaddle A, Stockwell T, Angus B, Cozzi-Lepri A, Delfino M, Dugan V *et al*: **Sequence Analysis of In Vivo Defective Interfering-Like RNA of Influenza A H1N1 Pandemic Virus**. *Journal of Virology* 2013, **87**(14):8064-8074.
23. Gomez-Puertas P, Albo C, Perez-Pastrana E, Vivo A, Portela A: **Influenza Virus Matrix Protein Is the Major Driving Force in Virus Budding**. *Journal of Virology* 2000, **74**(24):11538-11547.
24. Liu H, Grantham ML, Pekosz A: **Mutations in the Influenza A Virus M1 Protein Enhance Virus Budding To Complement Lethal Mutations in the M2 Cytoplasmic Tail**. *Journal of Virology* 2018, **92**(1):e00858-00817.
25. Wohlgemuth N, Ye Y, Fenstermacher KJ, Liu H, Lane AP, Pekosz A: **The M2 protein of live, attenuated influenza vaccine encodes a mutation that reduces replication in human nasal epithelial cells**. *Vaccine* 2017, **35**(48):6691-6699.
26. Grantham ML, Stewart SM, Lalime EN, Pekosz A: **Tyrosines in the Influenza A Virus M2 Protein Cytoplasmic Tail Are Critical for Production of Infectious Virus Particles**. *Journal of Virology* 2010, **84**(17):8765-8776.
27. Skehel JJ, Wiley DC: **Receptor Binding and Membrane Fusion in Virus Entry: The Influenza Hemagglutinin**. *Annual Review of Biochemistry* 2000, **69**:531-569.
28. Gamblin SJ, Skehel JJ: **Influenza Hemagglutinin and Neuraminidase Membrane Glycoproteins**. *Journal of Biological Chemistry* 2010, **285**(37):28403-28409.
29. Russell CJ, Hu M, Okda FA: **Influenza Hemagglutinin Protein Stability, Activation, and Pandemic Risk**. *Trends in Microbiology* 2018, **26**(10):841-853.
30. Suptawiwat O, Jeamtua W, Boonarkart C, Kongchanagul A, Puthawathana P, Auewarakul P: **Effects of the Q223R mutation in the hemagglutinin (HA) of egg-adapted pandemic 2009 (H1N1) influenza A virus on virus growth and binding of HA to human- and avian-type cell receptors**. *Acta Virologica* 2013, **57**(3):333-338.
31. Cotter CR, Jin H, Chen Z: **A Single Amino Acid in the Stalk Region of the H1N1pdm Influenza Virus HA Protein Affects Viral Fusion, Stability and Infectivity**. *PLoS Pathogens* 2014, **10**(1):e1003831.
32. Hannoun C: **The evolving history of influenza viruses and influenza vaccines**. *Expert Review of Vaccines* 2014, **12**(9):1085-1094.
33. **Key Facts About Seasonal Flu Vaccine** [https://www.cdc.gov/flu/protect/keyfacts.htm]
34. **How Influenza (Flu) Vaccines Are Made** [https://www.cdc.gov/flu/protect/vaccine/how-fluvaccine-made.htm]
35. Sridhar S, Brokstad KA, Cox RJ: **Influenza Vaccination Strategies: Comparing Inactivated and Live Attenuated Influenza Vaccines**. *Vaccines* 2015, **3**(2):373-389.

36. **Seasonal Influenza Vaccine Effectiveness, 2004-2018** [https://www.cdc.gov/flu/professionals/vaccination/effectiveness-studies.htm]
37. **Estimates of Influenza Vaccination Coverage among Adults—United States, 2017–18 Flu Season** [https://www.cdc.gov/flu/fluvaxview/coverage-1718estimates.htm]
38. **Estimates of Flu Vaccination Coverage among Children — United States, 2017–18 Flu Season** [https://www.cdc.gov/flu/fluvaxview/coverage-1718estimates-children.htm]
39. He W, Wang W, Han H, Wang L, Zhang G, Gao B: **Molecular Basis of Live-Attenuated Influenza Virus**. *PLoS ONE* 2013, **8**(3):e60413.
40. Maassab HF, Bryant ML: **The Development of Live Attenuated Cold-adapted Influenza Virus Vaccines for Humans**. *Reviews in Medical Virology* 1999, **9**:237-244.
41. Rudenko L, Yeolekar L, Kiseleva I, Isakova-Sivak I: **Development and approval of live attenuated influenza vaccines based on Russian master donor viruses: Process challenges and success stories**. *Vaccine* 2016, **34**(45):5436-5441.
42. MedImmune: **Highlights of Prescribing Information**. In. Gaithersburg, Maryland; 2018.
43. Gill MA, Schlaudecker EP: **Perspectives from the Society for Pediatric Research: Decreased Effectiveness of the Live Attenuated Influenza Vaccine**. *Pediatric Research* 2018, **83**(1):31-40.
44. Belshe RB, Edwards KM, Wesikari T, Black SV, Walker RE, Hultquist M, Kemble G, Connor EM: **Live Attenuated versus Inactivated Influenza Vaccine in Infants and Young Children**. *The New England Journal of Medicine* 2007, **356**:685-696.
45. Nichol KL, Mendelman PM, Mallon KP, Jackson LA, Gorse GJ, Belshe RB, Glezen P, Wittes J: **Effectiveness of Live, Attenuated Intranasal Influenza Virus Vaccine in Healthy, Working Adults: A Randomized Controlled Trial**. *JAMA* 1999, **282**(2):137-144.
46. Grohskopf LA, Sokolow LZ, Fry AM, Walter EB, Jernigan DB: **Update: ACIP Recommendations for the Use of Quadrivalent Live Attenuated Influenza Vaccine (LAIV4) — United States, 2018–19 Influenza Season**. *Morbidity and Mortality Weekly Report* 2018, **67**(22):643-645.
47. Poehling KA, Caspard H, Peters TR, Belongia EA, Congeni B, Gaglani M, Griffin MR, Irving SA, Kavathekar PK, McLean HQ *et al*: **2015–2016 Vaccine Effectiveness of Live Attenuated and Inactivated Influenza Vaccines in Children in the United States**. *Clinical Infectious Diseases* 2018, **66**(5):665-672.
48. Grohskopf LA, Sokolow LZ, Broder KR, Walter EB, Fry AM, Jernigan DB: **Prevention and Control of Seasonal Influenza with Vaccines: Recommendations of the Advisory Committee on Immunization Practices—United States, 2018–19 Influenza Season**. *Morbidity and Mortality Weekly Report* 2018, **67**(3):1-20.
49. McCown MF, Pekosz A: **The Influenza A Virus M2 Cytoplasmic Tail Is Required for Infectious Virus Production and Efficient Genome Packaging**. *Journal of Virology* 2005, **79**(6):3595–3605.

50. Neumann G, Watanabe T, Ito H, Watanabe S, Goto H, Gao P, Hughes M, Perez DR, Donis R, Hoffmann E *et al*: **Generation of influenza A viruses entirely from cloned cDNAs**. *PNAS* 1999, **96**(16):Generation of influenza A viruses entirely from cloned cDNAs.
51. Reed LJ, Muench H: **A Simple Method of Estimating Fifty Per Cent Endpoints**. *The American Journal of Hygiene* 1938, **27**(3):493-497.
52. Cox NJ, Kitame F, Kendal AP, Maassab HF, Naeve CW: **Identification of sequence changes in the cold-adapted, live attenuated influenzavaccine strain, A/Ann Arbor/6/60 (H2N2)**. *Virology* 1988, **167**:554-567.
53. Fischer II WA, King LS, Lane AP, Pekosz A: **Restricted replication of the live attenuated influenza A virus vaccine during infection of primary differentiated human nasal epithelial cells**. *Vaccine* 2015, **33**(36):4495-4504.

CURRICULUM VITAE

Laura M. Canaday

(815) 641-8486
lauracanaday23@gmail.com

EDUCATION

Expected May 2019 **Master of Science (ScM)**
Department of Molecular Microbiology and Immunology
Johns Hopkins Bloomberg School of Public Health,
Baltimore, MD
GPA: 3.67/4.0

August 2018 **Certificate in Vaccine Science and Policy**
Department of International Health
Johns Hopkins Bloomberg School of Public Health,
Baltimore, MD

May 2017 **Bachelor of Science (BS)**
Biology, The University of Alabama, Tuscaloosa, AL
Minor: Computer-Based Honors Program
GPA: 3.619/4.0, Cum Laude

RESEARCH EXPERIENCE

November 2017 – Present **ScM Thesis Research**
Johns Hopkins Bloomberg School of Public Health,
Baltimore, MD
Department of Molecular Microbiology and Immunology
Advisor: Dr. Andrew Pekosz, PhD

- Rescued H1N1 live, attenuated influenza vaccine viruses using a newly constructed M protein plasmid containing a novel mutation
- Perform a variety of assays, such as plaque assays and TCID50 assays, to compare wild type versus mutated viruses
- Utilize tissue cultures developed from patient human nasal epithelial cell samples
- Present data monthly at lab meetings for feedback and troubleshooting advice

August 2016 – May 2017 **Undergraduate Researcher**
The University of Alabama, Tuscaloosa, AL
Capstone College of Nursing
Advisor: Dr. Ann Graves, PhD, RN

- Measured spatial patterns of geographical accessibility to diabetes education services in adult Alabamian populations using GIS software
- Compared levels of accessibility across populations based on 5 characteristics in a retrospective cohort study of 4.8 million adults via U.S. Census data
- Conducted a systematic literature review to describe discrepancies in diabetes education services access across dozens of other regions

August 2014 – August 2016 **Undergraduate Researcher**
The University of Alabama, Tuscaloosa, AL
Department of Biological Sciences
Advisor: Dr. John Yoder, PhD

- Studied the effects of specific transcription factors on gene expression through genetic manipulation
- Established numerous colonies of hundreds *Drosophila melanogaster* flies with specifically manipulated genetic material to observe the effects of abdominal development based on transcription factor control
- Dissected and imaged hundreds of *Drosophila* pupae to analyze gene expression

ADDITIONAL EXPERIENCE

November 2018 – Jan. 2019 **Teaching Assistant**
Johns Hopkins Bloomberg School of Public Health, Baltimore, MD

- Grade 2 research proposals from over 50 students
- Facilitate discussions on an online forum for the class of 270

March 2018 – May 2019 **Insectary Staff**
Johns Hopkins Bloomberg School of Public Health, Baltimore, MD

- Clean trays used for mosquito egg hatching and larval growth

June 2014 - August 2014 **Howard Hughes Medical Institute Undergraduate Researcher**
The University of Alabama, Tuscaloosa, AL
Department of Biological Sciences
Advisor: Dr. John Yoder, PhD

- Completed a spring semester course in which students are encouraged to question critically and learn about the process of science

- Collaborated with a PhD candidate for 9 weeks in Dr. John H. Yoder's Development and Evolution lab investigating gene expression in *Drosophila melanogaster*
- Presented research at a poster session for fellow undergraduate students and departmental faculty
- Led to an invitation to continue as an undergraduate researcher with the Yoder lab

KEY SKILLS

Computer Skills: Microsoft Office; ArcGIS; NIS Elements Microscope Imaging; Photoshop
Microscopy: Scanning Electron (SEM); Transmission Electron (TEM); Imaging; Fluorescent
Cellular Biology: cell plating; bacterial sample staining; antibody staining; virus generation; cell culture; viral characterization assays (plaque assay, TCID50 assay)

PUBLICATIONS

Graves, B.A., Thompson, E., **Canaday, L.**, Liu, G., Bambis, B., & Kunberger, J. (2018), "Using Geographical Information Systems to Examine Access to Diabetes Self-Management Education Services in a Rural State." (In Review).

PRESENTATIONS

Graves, B.A., Thompson, E., **Canaday, L.**, Liu, G., Bambis, B., & Kunberger, J. *Using Geographical Information Systems to Examine Access to Diabetes Self-Management Education Services in a Rural State*. Podium presentation at the Capstone College of Nursing Research Colloquium, The University of Alabama, Tuscaloosa, AL. 2018.

Canaday, L., Thompson, E., Graves, B.A. *Access to Diabetes Healthcare Services: A Scoping Literature Review*. Poster presentation at the Undergraduate Research and Creative Activity Conference at The University of Alabama, Tuscaloosa, AL. 2017.

Canaday, L., Yoder, J.H. *Transcriptional Regulation of the Hox gene Abdominal-B*. Poster presentation at the Undergraduate Research and Creative Activity Conference at The University of Alabama, Tuscaloosa, AL. 2016.

Canaday, L., Yoder, J.H. *Exploring Enhancer Activity Surrounding Expression of the Sex-Determining Factor Doublesex*. Oral presentation for CBH Live at The University of Alabama Honors College, Tuscaloosa, AL. 2015.

Canaday, L., Wang, W., Yoder, J.H. *Exploring conserved enhancer activity of homologous wingless sequences between Drosophila melanogaster and virilis*. Poster presentation at the Undergraduate Research and Creative Activity Conference at The University of Alabama, Tuscaloosa, AL. 2015.

Canaday, L., Yoder, J.H. *Regulation between Hox proteins and the sex determining factor Doublesex*. Oral presentation for CBH Live at The University of Alabama Honors College, Tuscaloosa, AL. 2014.

SCHOLARSHIPS/FELLOWSHIPS

Fall 2018 - Spring 2019	Master's Tuition Reduction
Fall 2013 - Spring 2017	Computer Based Honors Fellowship
Fall 2013 - Spring 2017	Presidential Scholarship
April 2014	Dr. J. Henry Walker Memorial Scholarship in Biology

HONORS/AWARDS

Spring 2017	President's List
April 2017	Computer Based Honors Outstanding Senior
Spring 2016	Dean's List
April 2016	Computer Based Honors Outstanding Junior
April 2015	Computer Based Honors Outstanding Sophomore
Fall 2015	Dean's List
Spring 2014	Dean's List
Fall 2013	President's List

ORGANIZATIONAL INVOLVEMENT

January 2018 - Present	American Society for Microbiology
Spring 2016 - Present	Beta Beta Beta, National Biological Honor Society
Fall 2015 – May 2017	Section Leader, Million Dollar Band Clarinets
Spring 2014 – May 2017	Mentor, "Don't Try This at Home" Science Enrichment
Fall 2013 – Spring 2017	Member, Million Dollar Band